Degree Project in Sustainable Energy Engineering

Second cycle, 30 credits

Integrating Natural Refrigerant Heat Pumps into Existing Heating Networks

A Techno-Economic Study of Heat Pumps in District Heating Production

August Appelgren

Master of Science Thesis

Department of Energy Technology

KTH 2026

KTH Industrial Engineering and Management

Integrating Natural Refrigerant Heat Pumps into Existing Heating Networks

August Appelgren

Approved	Examiner	Supervisor
	Samer Sawalha	Arvid Johannisson
TRITA:	Industrial Supervisor	Contact person
TRITA-ITM-EX 2026:352	Jörgen Rogstam	August Appelgren

Abstract

Increasing biofuel resource competition leading to higher prices necessitate a diversification in Swedish district heating. This study presents a techno-economic evaluation of integrating a 15 MW air-source heat pump into an existing urban district heating network in electricity bidding zone SE4. To ensure environmental sustainability and alignment with tightening EU regulations, four natural refrigerants within three different thermodynamic configurations are investigated. A time-resolved, deterministic simulation framework is developed using Python to model the hourly thermodynamic performance of a two-stage ammonia cycle, a two-stage hydrocarbon cascade cycle, and a one-stage carbon dioxide ejector cycle against real-world network temperature and hourly electricity market profiles from 2025. Beyond traditional fuel substitution, the model integrates flexibility revenues from the mFRR balancing market. The results demonstrate the thermodynamic and economic superiority of the two-stage ammonia system, achieving the highest efficiency with an average operating COP of 3.22 and total annual net savings of 17.5 MSEK. The hydrocarbon cascade system performs closely, yielding 16.3 MSEK in net savings and proving highly viable under wide temperature lifts. Conversely, the transcritical carbon dioxide system underperforms within existing high-temperature network regimes due to a severe gas-cooling thermal bottleneck. Sensitivity analyses reveal that the investment viability is primarily governed by biofuel procurement prices and electricity price volatility. Furthermore, the results indicate that ancillary market participation acts as a critical economic lever by lowering electricity-to-fuel price parity thresholds.

Sammanfattning

Som ett resultat av hårdnad konkurrens om biobränslen har priset på skogsflis stigit med nära 100% under perioden 2022 till 2025, varpå en diversifiering av produktionsmixen i svensk fjärrvärmeproduktion är efterfrågad. Denna studie undersöker de tekniska och ekonomiska förutsättningarna för att integrera en luftvärmepump på 15 MW i ett befintligt fjärrvärmenät i elområde 4. För att ligga i linje med skärpta miljökrav från EU utvärderas endast naturliga köldmedier. Inom ramen för projektet har en simuleringsmodell utvecklats i Python, där modellen beräknar den timvisa termodynamiska prestandan för tre olika systemlösningar: en tvåstegs ammoniakcykel, en tvåstegs kaskadcykel med kolväten samt en enstegs koldioxidcykel med ejektor. Simuleringarna bygger på faktiska framlednings- och returtemperaturer samt timvisa elmarknadsdata från 2025. Utöver att beräkna den rena bränslebesparingen simulerar modellen även potentiella intäkter från balanseringsmarknaden för manuell frekvensåterställningsreserv (mFRR). Resultaten visar att tvåstegssystemet med ammoniak är det bästa alternativet, både tekniskt och ekonomiskt. Det ger högst effektivitet med ett genomsnittligt COP på 3,22 och en årlig nettobesparing på 17,5 MSEK. Kolvätekaskaden presterar nästan lika bra (16,3 MSEK i nettobesparing) medan koldioxidsystemet relativt sett underpresterar i det nuvarande högtemperaturnätet. Avslutningsvis visar känslighetsanalyserna att lönsamheten i investeringen framför allt styrs av priset på det alternativa bränslet (biomassa) samt elpriset. Att delta på stödtjänstmarknaden fungerar dock som en viktig ekonomisk hävstång, eftersom det sänker tröskeln för när eldriften blir mer lönsam än eldning av biobränsle.

Acknowledgements

Firstly, I would like to thank my two supervisors Samer and Arvid at KTH, who have been a valuable support during the entire process. Thank you for being so interested in my work and helping me forward with your expertise and passion. I would also like to thank my industrial supervisor Jörgen, for giving me the opportunity to do my thesis in collaboration with him and the rest of the people at EKA. Your drive and curiosity have been a major reason why this work has been so enjoyable and is something that I will carry with me in the future. Lastly, thank you to my friends and family for being curious about my progress and such a joy to spend time with in between the simulations.

Table of Contents

List of Figures

List of Tables

Abbreviations

CAPEX	Capital Expenditure
COP	Coefficient of Performance
DSO	Distribution System Operator
DH	District Heating
ETS	Emissions Trading System
EU	European Union
F-Gas	Fluorinated Gas
GWP	Global Warming Potential
HEX	Heat Exchanger
HP	Heat Pump
IEA	International Energy Agency
mFRR	manual Frequency Restoration Reserve
NPV	Net Present Value
OCB	Operational Cost Boiler
OCHP	Operational Cost Heat Pump
OPEX	Operational Expenditure
SCOP	Seasonal Coefficient of Performance
TSO	Transmission System Operator
VRE	Variable Renewable Energy

Nomenclature

Sign	Description	Unit
Q	Heat Energy	J
W	Electrical Work	J
COP_{Carnot}	Coefficient of Performance for Carnot Cycle	-
T_{hot}	High Temperature Reservoir	K
T_{cold}	Low Temperature Reservoir	K
$T_{sat,evap}$	Saturation Temperature during Evaporation	K
T_{source}	Heat Source Temperature	K
T_{sink}	Heat Sink Temperature	K
$\Delta T_{approach}$	Temperature Difference at Inlet	K
$\Delta T_{superheat}$	Temperature Change due to Superheating	K
ΔT_{pinch}	Temperature Difference at Pinch Point	K
$T_{refrigerant}$	Refrigerant Temperature	K
P_1	High Pressure	Pa
P_2	Low Pressure	Pa
Π	Pressure Ratio	-
$\eta_{is,tot}$	Total Isentropic Efficiency	-
η_{vol}	Volumetric Efficiency	-

1 Introduction

The opening chapter outlines the motivations for transitioning toward large-scale heat pumps within the Swedish district heating sector, specifically focusing on the shift from biomass combustion to electrified solutions. It defines the underlying challenges with fuel price volatility, establishes the study's primary objectives, and presents the research questions.

1.1 Background

Historically, the Swedish district heating system has relied heavily on combustion, with biofuels playing a pivotal role in the phase-out of fossil fuels [1]. Despite the historical importance of biofuels, recent market developments have created uncertainty regarding their future availability. Increased competition for biomass from other sectors, coupled with geopolitical factors, has led to higher prices, challenging the profitability of combustion-based heat production [2]. In response to these challenges, electrification via large-scale heat pumps has been identified as a key strategy for diversifying production portfolios. By utilizing power to heat technologies, district heating systems cannot only reduce their dependence on combustion but also serve as a flexibility resource in an electrical grid with a growing share of variable renewable energy [3].

The diversification with heat pumps does involve critical technical and environmental choices. The European Union's tightened regulation regarding fluorinated gases is driving a phase-out of synthetic refrigerants with high global warming potential (GWP), making natural refrigerants a future-proof alternative [4]. Simultaneously, electrification introduces a new economic dimension: the operational expenditure (OPEX) of the heat pump becomes directly linked to the volatile electricity market. Electricity prices fluctuate significantly depending on weather conditions and grid load, necessitating advanced operating strategies to optimize production against spot prices and potential balancing services [5]. For large-scale heat pumps to become an economically viable replacement for biomass-fired heat, a deeper understanding is required of how technical performance interacts with the dynamic price signals of the electricity market.

1.2 Collaborating Partner

This thesis project is carried out in collaboration with EKAnalys AB (EKA), a Swedish consultancy firm specializing in refrigeration and heat pump technology. EKA provides technical expertise and analysis for complex energy systems, helping clients optimize performance and transition toward sustainable solutions. To ensure practical and industrial relevance, this study is conducted as a case study centred on a specific district heating production facility. EKA has previously performed technical assessments for the plant, providing a foundation of operational insights and data that this thesis builds upon. The results of this study are intended to support the further development of EKA's analytical toolbox by providing a methodology for integrating dynamic electricity price data and detailed performance mapping of natural refrigerants.

1.3 Problem Statement

The transition towards a more electrified and integrated energy system introduces a complex dependency between heat production and the electricity market. While biomass remains a cornerstone of Sweden's district heating supply, increasing resource competition has created a need for greater operational flexibility. Unlike traditional boilers, the OPEX of a heat pump is governed by a highly volatile energy market, making the economic viability of electrification highly sensitive to market dynamics.

However, integrating technical performance with this market volatility remains a significant challenge for energy system analysts. Many current evaluation methods rely on simplified assumptions, such as static coefficient of performance (COP) values or average annual electricity prices, which fail to capture the reality of modern, highly dynamic energy markets. A more robust framework is required to bridge the gap between technical and economic dimensions. It involves simultaneously accounting for the technical variability of natural refrigerants under varying temperature profiles, and the multifaceted cost structure of electricity. Without such an integrated approach, there is a risk of suboptimal investment decisions and a missed opportunity to utilize balancing resources in the energy system, which is essential for optimizing renewable energy assets.

1.4 Aim and Research Questions

The primary aim of this thesis is to evaluate the technical and economic viability of large-scale heat pumps as a partial replacement for biomass-fired heat production in Swedish district heating, specifically accounting for hourly electricity market dynamics.

To fulfil this aim, the following research questions will be addressed:

1. Which of the selected natural refrigerant cycles achieves the highest COP under various heat source and heat sink conditions in Sweden?

2. How does the justified capital expenditure vary between the selected refrigerant cycles, and which economic parameters most significantly influence this investment threshold?

3. What are the price ratio thresholds between electricity and biofuel at which the production cost of the heat pump equals that of biomass boilers?

1.5 Objectives

The objectives of the study are the following:

1. Perform thermodynamic modelling of heat pump cycles with carbon dioxide (R744), propane (R290), isobutane (R600a), and ammonia (R717) to map COP across varying source and sink temperatures.

2. Gather and process data for electricity spot prices, grid fees, and taxes.

3. Develop a time-resolved simulation framework that integrates the thermodynamic performance maps with the dynamic electricity cost components.

4. Determine the production cost parity points relative to current biofuel price benchmarks.

5. Conduct a sensitivity analysis to assess how variations in future fuel and electricity prices impact the economic viability.

1.6 Scope and Limitations

The scope of this study is addressed on a comparative analysis of different heat pump configurations and their respective natural refrigerant(s), specifically evaluated within the context of the Swedish energy system. To maintain a rigorous focus, the systems are modelled based on fundamental thermodynamic cycles and regression-based performance data, rather than addressing detailed mechanical design, component-level fluid dynamics, or the long-term chemical stability of the refrigerants under high-temperature stress. This choice is deliberate, as it allows the study to prioritize system-level performance and economic viability over mechanical engineering specifics. A key technical limitation involves the reliance on manufacturer-provided data for compressors. Since manufacturer's catalogues often restrict the operational envelope for refrigerants at high delivery temperatures, this study utilizes mathematical extrapolation based on pressure ratios to estimate performance beyond these limits. It is therefore assumed that mechanical hardware capable of withstanding the resulting pressures is available, although the site-specific mechanical longevity and lubrication requirements under these conditions are not explicitly modelled.

Furthermore, the analysis is strictly focused on the heat pump unit itself and its immediate integration into the district heating network. Consequently, the complex hydraulic dynamics, piping losses, and insulation characteristics of the wider district heating grid are considered outside the scope. The heat source is limited to ambient air, and while seasonal temperature variations are included, the model does not account for local microclimate variations or potential airflow interference between multiple units in a large-scale installation. On the economic side, the study is restricted to the Swedish electricity market, incorporating taxes, grid fees, and power demand charges utilized by one of the major grid operators. While the model includes auxiliary revenue streams from the manual frequency restoration reserve (mFRR) market to reflect modern grid-stabilization strategies, it does not simulate the increased mechanical wear and tear, or the potentially shortened maintenance intervals caused by the frequent ramping and cycling of the compressor. Finally, simulations are conducted with an hourly resolution, consequently leading to sub-hourly fluctuations and long-term multi-decadal climate projections not being included.

2 Background

This section establishes the theoretical framework for heat pump technology and natural refrigerants while providing an overview of the Swedish electricity market dynamics.

2.1 Electricity Market Architecture

The Nordic electricity market is built upon a zonal pricing model, coordinated through the regional power exchange Nord Pool. In this architecture, the physical power system is divided into distinct bidding zones, which serve as the primary tool for managing structural congestion within the transmission grid. Sweden is currently divided into four bidding zones, designated SE1 to SE4, ranging from the hydropower-rich northern regions to the high-demand areas in the south. As illustrated in Figure 1, these zones allow the market to reflect the physical reality of the grid, where electricity prices diverge when transmission constraints between zones are reached [1], [2].

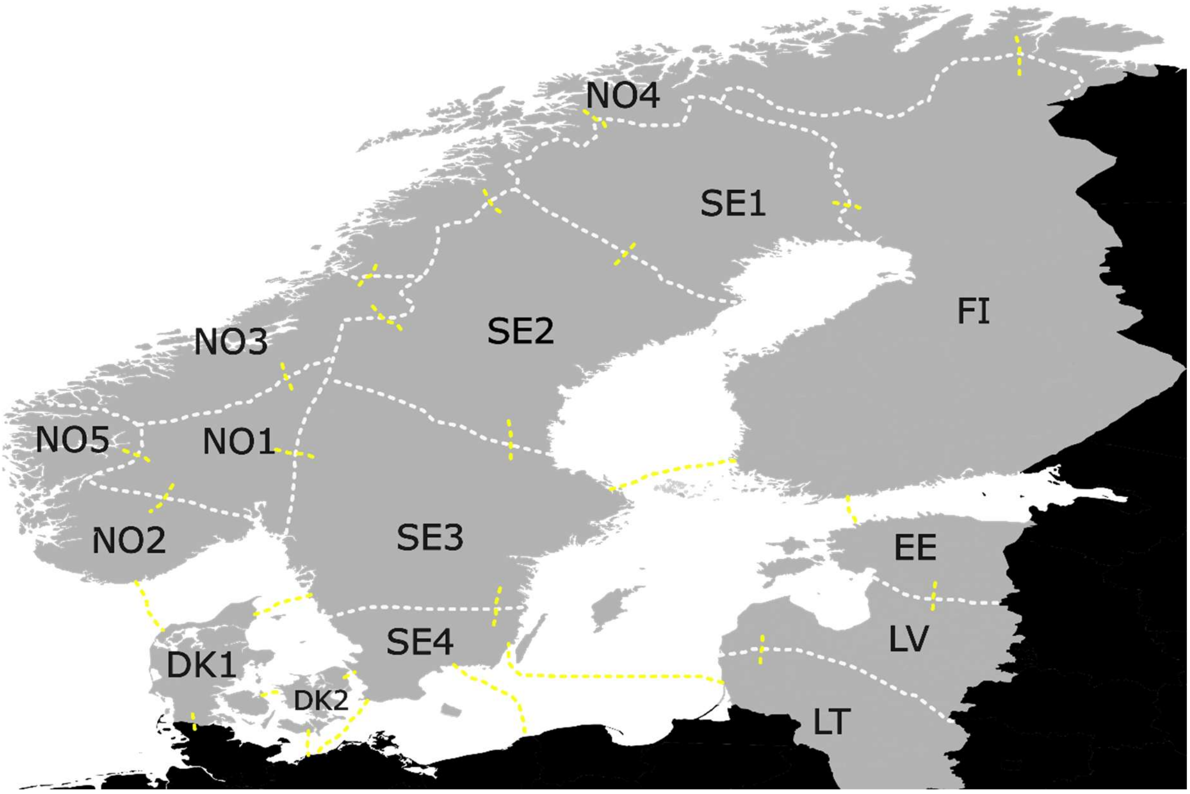

Figure 1: Nordic bidding zones and major transmission interconnectors (yellow lines).

The administrative and technical oversight of the Swedish market is managed by the transmission system operator (TSO), Svenska Kraftnät, which is responsible for defining the boundaries and transfer capacity between the zones. The zonal configuration is intended to provide locational price signals that incentivize both production and consumption to support grid stability [3]. Recent studies highlight that while zonal systems aim for price convergence, significant price wedges frequently occur between northern (SE1, SE2) and southern Sweden (SE3, SE4) due to internal bottlenecks and transfer capacity to the European continent [2].

The day-ahead market is the primary venue for electricity trading, where prices are determined quarterly through a blind auction process based on the intersection of supply and demand. In this process, the market operator calculates a system price (a theoretical price assuming no transmission constraints) as well as the specific area prices for each bidding zone [4]. As shown in Table 1, the divergence between the system price and the local area price in SE3 or SE4 can be substantial, directly impacting the operational threshold for power to heat technologies [5].

Table 1: Historical electricity spot price development (yearly average). Data sourced from Nord Pool [6].

Year	System Price [SEK/MWh]	SE1 [SEK/MWh]	SE2 [SEK/MWh]	SE3 [SEK/MWh]	SE4 [SEK/MWh]
2021	633.8	432.3	432.9	671.6	818.7
2022	1446.5	634.1	664.3	1378.7	1620.5
2023	643.2	455.8	455.9	589.8	741.6
2024	411.7	285.7	280.9	408.8	568.5
2025	439.9	185	183.1	512.4	669.6

2.2 Pricing Mechanisms

The fundamental mechanism for price formation in the nordic market is based on the principle of marginal pricing, often referred to as the pay-as-cleared model. In this system, all electricity generators within a bidding zone receive the same price for their production, which is determined by the marginal cost of the last unit of production required to meet the total demand. This creates a supply curve, known as the merit order, where technologies with low variable costs (such as wind and solar power) are dispatched first, while plants with higher marginal costs (typically fossil-fuelled or biomass-based thermal plants) are called upon only when demand increases [5], [7].

The introduction of variable renewable energy (VRE) has a profound impact on this curve, a phenomenon known as the merit order effect, illustrated in Figure 2. When production from wind or solar is high, these near-zero marginal cost sources shift the supply curve to the right, effectively displacing more expensive thermal production and lowering the equilibrium price [8]. In a study of the Swedish bidding zones, it's demonstrated that this effect is particularly strong in regions with high wind penetration, often leading to periods of low or even negative electricity spot prices [5]. For a large-scale heat pump, these periods represent the most economically favourable operating conditions, as the marginal cost of heat production becomes a fraction of that from competing biofuel boilers.

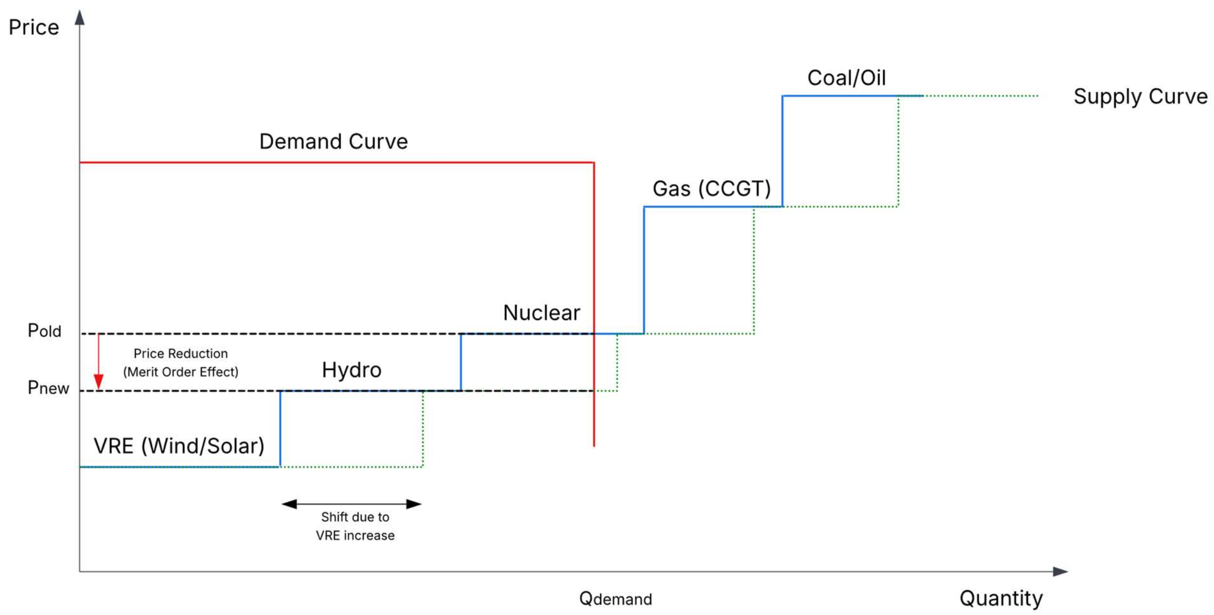

Figure 2: Conceptual illustration of the merit order effect in the Nord Pool electricity market.

Historically, the market has operated with hourly resolution. However, in line with the harmonised imbalance settlement project in the EU, the Swedish market transitioned to a 15-minute time resolution in October 2023 for imbalance settlement, with the full integration into the day-ahead market following in late 2025. This shift to a 15-minute imbalance settlement period allows the market to better reflect the rapid fluctuations of intermittent production and demand. For the techno-economic modelling of heat pumps, this higher resolution is critical, as it captures short-term price spikes and dips that were previously smoothed out in hourly averages, potentially increasing the value of operational flexibility [3], [9]. The merit order is also influenced by the price of carbon dioxide emission allowances within the EU's emissions trading system. Even though the Swedish production mix is largely fossil-free, the price in southern Sweden (SE3 and SE4) is frequently set by interconnectors to continental Europe or the Baltics, where fossil-fuelled plants are more prevalent. Consequently, high carbon prices on the continent can spill over into Swedish bidding zones, raising the electricity price and affecting the parity point between electrified heat and local biomass combustion [10].

2.3 Price Volatility

The rapid expansion of VRE, particularly wind power, has fundamentally altered the volatility profile of the nordic electricity market. While traditional production mixes dominated by hydro and nuclear power provided a relatively stable price floor, the stochastic nature of wind and solar generation introduces significant short-term fluctuations [7]. In the Swedish market, this volatility is characterized by an inverse relationship between wind speed and spot prices; during periods of high wind speed, the supply curve shifts so far to the right that prices can drop toward zero or even become negative, a phenomenon increasingly observed in bidding zones SE3 and SE4 [5]. This correlation is visualized in Figure 2, which illustrates how increased wind power penetration leads to a compression of the market price.

The integration of VRE not only impacts the price level locally but also increases volatility spillovers between interconnected markets. For the Swedish system, this means that price spikes or dips in continental Europe are more easily transmitted to the Swedish bidding zones when production contains intermittent sources [11]. It's emphasized that while hydropower-rich areas like SE1 and SE2 exhibit lower volatility due to the inherent storage capacity of reservoirs, the southern zones are more exposed to the price jumps associated with sudden changes in weather conditions [12]. A critical aspect for the operational strategy of large-scale heat pumps is the intraday price spread. High volatility creates a high price-to-price ratio between peak and off-peak hours, allowing the heat pump to time its consumption to periods where electricity is cheaper than the equivalent energy from biomass combustion [7]. As seen in Figure 3, the frequency of hours with extreme price volatility has increased significantly over the last decade, reinforcing the economic case for flexible power to heat solutions. Coefficient of variation is defined as the ratio of the standard deviation to the mean of electricity spot price.

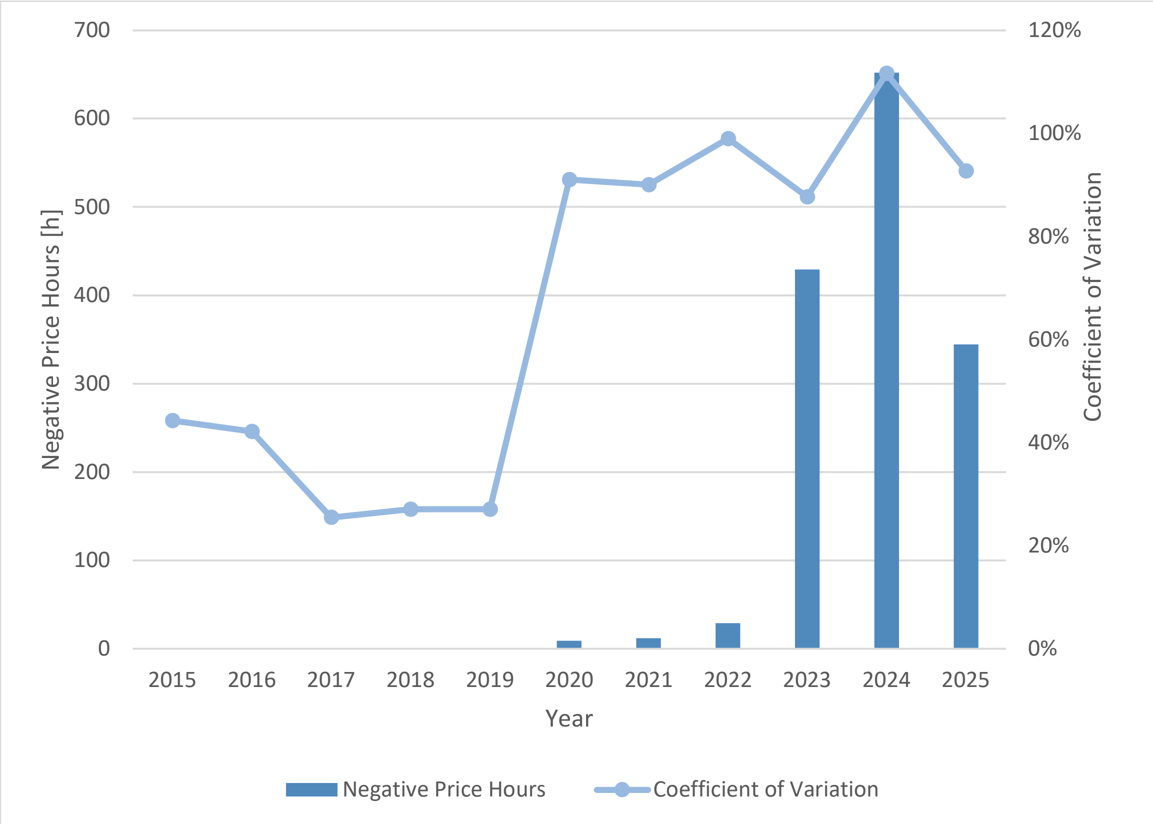

Figure 3: Historical development of spot price volatility and negative price occurrences in bidding zone SE3. Data compiled from ENTSO-e [6].

Furthermore, the duration of these low-price periods is essential for the technical viability of the heat pump. If low-price windows are too short, the thermal inertia of the district heating network and the ramp-up times of the heat pump units may limit the system's ability to respond to market signals [13]. Therefore, the profitability of the investment is highly sensitive not only to the average electricity price but to the frequency and magnitude of the extreme volatility events caused by intermittent production [12].

2.4 Grid Fees and Power Tariffs

The Swedish electricity grid is a regulated natural monopoly where distribution is overseen by the Swedish Energy Markets Inspectorate to ensure fair and transparent pricing [3]. For industrial-scale energy consumers, such as the large-capacity heat pump systems analysed in this study, grid fees represent a significant component of the operational expenditure. These fees are designed to provide price signals that encourage consumers to shift their load away from periods when the grid is heavily congested, thereby ensuring system stability [14]. In high-voltage industrial contracts, this is typically achieved through a combination of power-based and energy-based charges that vary depending on the time of day and season.

A characteristic high-voltage tariff, such as the Vattenfall N2T model used in this study, utilizes a time-differentiated energy transmission charge in addition to fixed and power-based fees [15]. The transmission charge is often significantly higher during peak-load hours, which in Sweden generally occur during winter weekdays when the total national demand is at its peak. Simultaneously, the tariff includes a monthly power demand charge based on the highest hourly average peak, along with an additional peak-load power fee during the coldest months [15]. This dual structure, where the cost of energy consumed as well as the cost of the maximum power capacity utilized depend on the timing of the withdrawal, creates a complex optimization environment. Integrating these time-sensitive grid costs into the modelling procedure is essential for a realistic assessment of heat pump dispatch. It should be noted that while this study adopts a specific tariff structure as a reference, the exact balance between power-based and energy-based charges varies between different regional grid operators, making the local grid conditions a decisive factor in the economic feasibility of large-scale heat pump integration.

2.5 Ancillary Services and Grid Balancing

As the energy system transitions towards a higher share of intermittent renewable generation, such as wind and solar power, the inherent rotational inertia of the grid decreases. This shift creates a greater need for ancillary services to maintain the frequency balance between generation and demand [16]. In Sweden, the market for these balancing services has expanded rapidly, with the total turnover increasing from approximately 1.6 billion SEK in 2020 to over 6 billion SEK in 2022 [17]. These services are categorized into several products depending on their response time and purpose, ranging from automatic frequency containment reserves to manual restoration reserves.

For large-scale heat pumps, the manual frequency restoration reserve (mFRR) is of particular interest due to its longer response time relative to other markets. The choice to focus on mFRR is primarily driven by its operational requirements, as it allows for a longer activation time compared to the near-instantaneous response required by fast frequency reserves [16]. The larger timeframe is technically compatible with the ramping capabilities of industrial heat pump units and the operational coordination required within a heating plant. The market is structured as a two-stage sequential process involving both readiness and physical delivery, as illustrated in Figure 4. The first stage consists of the capacity market, where resources are remunerated for being available to the TSO, ensuring that sufficient reserves are secured in advance. The second stage is the activation market, which handles the real-time energy delivery when a frequency deviation occurs. As shown in the figure, both stages are bifurcated into upward and downward regulation, allowing the TSO to address both undersupply and oversupply in the grid.

In this context, the flexibility of the heat pump is often facilitated through sector coupling between the electricity and thermal sectors. Rather than relying solely on the thermal inertia of the buildings or the network, a hybrid heating plant can utilize another heat source, such as a biomass boiler, to compensate for the reduced output of the heat pump during upward regulation events [18], [19]. This strategic shift between energy carriers allows the facility to provide grid stabilization services without compromising the heat delivery to the end-users. Consequently, the integration of mFRR revenues into the techno-economic assessment transforms the heat pump from a pure heating asset into a dynamic participant in the balancing market, potentially enhancing project profitability in price-volatile regions [17].

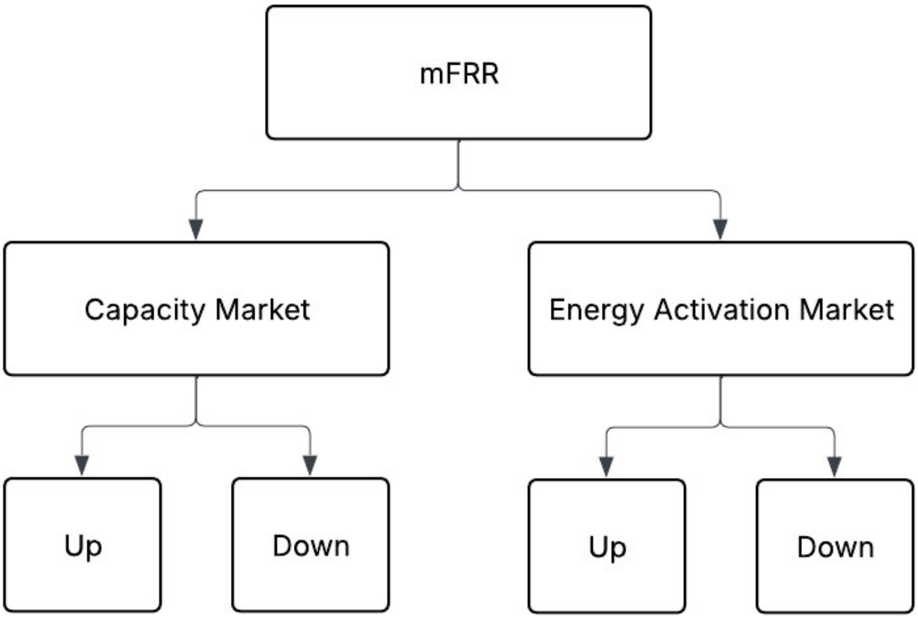

Figure 4: Schematic of the mFRR market structure.

2.6 The Vapor Compression Cycle

The fundamental principle of a heat pump is the vapour compression cycle, a thermodynamic process designed to transfer thermal energy from a lower-temperature source to a higher-temperature sink through the application of mechanical work [20]. In district heating applications, this cycle is utilized to upgrade low-grade heat to temperature levels suitable for space heating and domestic hot water production. While large-scale heat pumps can technically recover energy from various sources, such as sewage water or industrial excess heat, this study focuses exclusively on ambient air as the primary heat source. This choice is motivated by the universal availability of air, which ensures that the results of the modelling are not constrained by specific local geographical or industrial prerequisites, unlike water or waste heat based systems [14].

The performance of the vapour compression cycle is heavily dependent on the temperature of the heat source, as the temperature difference between the source and the sink directly dictates the pressure ratios required and, consequently, the compressor's energy consumption [21]. Utilizing ambient air introduces a specific dynamic challenge, as the source temperature fluctuates seasonally and daily, often reaching its lowest points when the heating demand is at its peak. Therefore, understanding the transient behaviour and efficiency characteristics of the cycle under varying ambient conditions is essential for accurately evaluating the heat pump's role in a flexible energy system [22].

The main stages in the vapour compression cycle are as follows:

1. **Evaporation:** The refrigerant enters the evaporator as a low-pressure mixture of liquid and vapour. By absorbing heat from the external source, the refrigerant undergoes a phase change into a vapour. The temperature of the source must remain higher than the refrigerant's boiling point to ensure effective heat transfer, thus dictating the evaporation pressure [20], [21].
2. **Compression:** The saturated or slightly superheated vapour is suctioned into the compressor. Mechanical work is applied to raise the pressure and, consequently, the temperature of the gas. While ideally modelled as an isentropic process, real-world compression involves internal friction and heat losses, affecting the discharge temperature [20], [23], [24].
3. **Condensation:** The high-pressure and high-temperature gas enters the condenser, where it rejects heat to the sink. During this process, the refrigerant condenses back into a liquid state. In large-scale systems, the condenser is often designed to allow for subcooling of the liquid to improve the cooling capacity in the next stage [25], [26].
4. **Expansion:** The high-pressure liquid passes through an expansion valve or throttling device. This process causes a rapid drop in pressure, resulting in a decrease in temperature, returning the refrigerant to a low-pressure state ready to re-enter the evaporator [20].

2.7 Efficiency and Temperature Lift

The performance of a heat pump is primarily evaluated through the COP, which defines the ratio of the useful heat delivered to the sink to the electrical work required by the compressor [21], [25]. For large-scale applications, maximizing this ratio is essential to ensure that the technology remains economically competitive against combustion-based alternatives. This fundamental relationship is expressed as in Equation 1:

$$COP = \frac{\dot{Q}_{hot}}{\dot{W}} \tag{1}$$

While the above equation describes the operational efficiency, the second law of thermodynamics dictates an upper theoretical limit for any heat pump cycle, known as the Carnot COP [20], [23]. This limit represents a perfectly reversible cycle and is determined solely by the absolute temperatures (in Kelvin) of the heat source and the heat sink:

$$COP_{Carnot} = \frac{T_{hot}}{T_{hot} - T_{cold}} \tag{2}$$

In practical applications, the actual COP is always lower than the Carnot limit due to unavoidable technical losses. These include mechanical friction in the compressor, electrical losses in the motor, and the temperature differences required across the heat exchanger surfaces to drive the heat transfer [23], [26]. A critical takeaway from the Carnot equation is the impact of the temperature lift (the gap between source and sink temperatures). As the required temperature lift increases, the compressor must perform more work per unit of heat delivered, leading to a significant decline in COP [21], [26]. This relationship is central to the techno-economic modelling in this study, which illustrates how the efficiency drops as the supply temperature rises relative to a constant heat source.

2.8 Working Fluids and Refrigerants

The selection of an appropriate working fluid is a critical factor in the design and optimization of heat pump and refrigeration systems. With increasing environmental regulations, such as the f-gas regulation and the Kigali Amendment to the Montreal Protocol, the industry is transitioning toward natural refrigerants [27], [28]. This section examines the characteristics of the selected natural refrigerants:

R744 (Carbon Dioxide):

R744 is a non-flammable and non-toxic natural refrigerant with a GWP of 1. Due to its low critical temperature (31.1 °C), R744 typically operates in a transcritical cycle where heat rejection occurs above the critical point [29], [30]. While this leads to high operating pressures, often exceeding 100 bar, the transcritical operation results in a significant temperature glide during gas cooling. To maximize the COP, modern R744 systems often utilize multi-stage compression or an ejector to mitigate expansion losses [30], [31].

R290 (Propane):

R290 is a hydrocarbon refrigerant with a relatively low GWP of less than 3. It serves as a viable alternative to R134a (tetrafluoroethane) due to its similar pressure levels and high latent heat of vaporization, which contributes to high system efficiency. However, R290 is classified as highly flammable, which introduces safety challenges [32], [33], [34].

R600a (Isobutane):

Commonly used in domestic refrigeration, R600a is another hydrocarbon with minor environmental impact. Compared to R290, R600a operates at lower pressures, which allows for quieter operation and reduced mechanical stress on compressor components. A critical performance factor for R600a systems is the impact of air impurities; studies show that even small mass fractions of air can significantly hinder heat transfer during condensation and reduce overall energy efficiency. Furthermore, R600a has an evaporation limit at approximately -10 °C due to the pressure getting close to atmospheric pressure [35], [36].

R717 (Ammonia):

R717 is often seen as one of the most efficient refrigerants for large-scale applications. It offers superior heat transfer coefficients and a high COP with zero ozone depletion- and global warming potential. While highly efficient, R717 is toxic and mildly flammable, requiring stringent safety protocols and well-ventilated installations [20], [28], [31].

2.9 Related Works

The integration of large-scale heat pumps within district heating networks has been extensively studied from various macro-systemic perspectives. A certain study provided a comprehensive historical and status review of the Swedish district heating sector, documenting the massive deployment of large heat pumps during the 1980s and establishing their competitive advantage due to low specific investment costs and the ability to utilize low-cost surplus electricity [37]. On a European scale, another study has quantified the future potential within the Heat Roadmap Europe framework, projecting that large-scale heat pumps should supply approximately 25-30% of the entire district heating demand by 2050 to achieve decarbonization targets [38]. Furthermore, the positioning and hydraulic connection of these assets within the network grids, such as assessing the trade-offs between utilizing supply or return lines, have been systematically categorized, emphasizing the thermal barriers imposed by traditional high-temperature networks [39].

While the existing literature firmly establishes the systemic benefits and macro-economic potential of large-scale heat pumps, a significant research gap remains concerning the granular intersection of advanced natural refrigerant configurations and real-time electricity market dynamics. Many current techno-economic evaluations rely on static or averaged electricity price profiles and treat the heat pump as a static thermal generator operating at fixed grid conditions. There is a lack of comprehensive comparative research evaluating how thermodynamic cycles perform when dynamically operated against both highly volatile spot market prices and auxiliary revenue mechanisms like the manual frequency restoration reserve market.

3 Methodology

This chapter establishes the overarching methodological framework designed to address the study's objectives. While the technical specifics and mathematical formulations of the simulation model are detailed in Chapter 4, this section outlines the high-level progression from literature synthesis to physical and economic evaluation, employing a case study driven approach to ensure practical relevance.

3.1 Research Approach

The study adopts a quantitative research approach based on mathematical modelling and deterministic simulations of physical systems. The core of the methodology involves simulating the thermodynamic performance of various heat pump cycles and integrating these technical results with historical market data. By combining physical laws with empirical economic data, the approach enables a holistic evaluation of how refrigerant properties and system configurations impact long-term financial viability in a fluctuating energy landscape.

3.2 Data Collection and Processing

The simulation relies on input data and thermophysical properties from several sources:

- **Market Data:** Historical hourly electricity spot prices and balancing market data (mFRR) from 2025 were collected from ENTSO-e and Svenska Kraftnat respectively, to reflect real-world market conditions.
- **Refrigerant Properties:** Thermophysical data for the investigated refrigerants were sourced from an established property library named CoolProp to ensure accurate cycle calculations.
- **District Heating Profiles:** Actual temperature profiles from the investigated district heating network were utilized. This includes hourly data for supply and return temperatures, as well as heat source temperatures in terms of ambient air, allowing the model to reflect the specific temperature lifts required by the system throughout a full operating year.

Missing data and outliers in the input data set were handled by imputation. The exact methods used were forward and backward fill, since the data occurred as a time series. Furthermore, the reason why 2025 was chosen as simulation year was to capture the new market landscapes for both electricity and biofuel. The price of wood chips, a common type of biofuel, has close to doubled during the period 2022 to 2025, reaching a level never seen before [40]. Simultaneously, the electricity spot market has entered a new landscape too. Prices are significantly more volatile compared to earlier, seen in Figure 3.

3.3 Simulation and Evaluation Framework

The simulation was implemented using Python, structured to link technical performance directly to economic outcomes. The logical path follows a sequential flow:

1. **Technical Module:** Calculates the hourly COP and heating capacity based on the specific refrigerant cycle and current temperature conditions.
2. **Dispatch Logic:** An hourly decision-making algorithm determines whether to operate the heat pump or not based on production costs.
3. **Economic Module:** Aggregates the hourly results into annual net savings, accounting for energy displacement, power tariffs, and mFRR revenues.

A case study approach was selected to validate the model within a real-world context. By applying the simulation to an existing district heating plant, the results can be compared with actual operating conditions and constraints, ensuring that the theoretical findings are grounded in practical industrial requirements.

3.4 Validation

To strengthen the reliability of the study, the thermodynamic model's technical outputs were cross-referenced with results from similar cycles in alternative software environments where possible. It was only managed to be done for the carbon dioxide cycle, using the software Simple One Stage CO2 Cycle developed by the company IPU. Furthermore, the robustness of the economic findings was evaluated through a sensitivity analysis. By varying key parameters, such as biofuel price and electricity spot price, the analysis identified which factors pose the greatest risk to the investment and ensured that the conclusions remained valid under shifting market conditions. The analysis examined how variations in key economic and technical parameters impact the justified CAPEX. Five parameters were varied up and down respectively while keeping all other variables constant, examining how the justified CAPEX would be affected.

4 Modelling

The focus in this chapter is on the technical and economic characterization of the selected heat pump systems and their integration into the energy model. All thermodynamic assumptions, refrigerant-specific configurations, and algorithm for operation are detailed within this section.

4.1 Two-Stage Ammonia Cycle

The ammonia system is designed as a two-stage compression cycle to handle the required pressure ratios at high temperature lifts. A key feature of this configuration is the heat provision strategy involving the district heating (DH) return water. Upon entering the system, the DH return flow is split into two parallel branches. One branch passes through the main condenser, while the other passes through a dedicated inter cooler located after the low-pressure compressor (see Figure 5). This arrangement ensures that both components receive water at the same return temperature, maximizing the cooling potential of the hot discharge gas. Following the inter cooler, the refrigerant is further cooled in a flash tank before entering the second compression stage.

On the low-pressure side, a flooded evaporator configuration is employed, which interacts with the heat source via an intermediate loop and an external heat exchanger. This design choice is a critical safety measure driven by the thermodynamic and chemical properties of ammonia. Direct heat extraction from the source would require a substantially larger charge of the toxic and mildly flammable refrigerant, vastly increasing the facility's risk profile and complicating compliance with strict safety distances and urban zoning regulations. In this setup, the evaporator is fed from a surge drum (separator), ensuring that the internal heat transfer surfaces remain fully wetted by liquid refrigerant. This maximizes the evaporation heat transfer coefficient and improves the overall efficiency compared to a dry expansion system. The separator ensures that only dry vapor, in this model considered as saturated vapor, reaches the suction line.

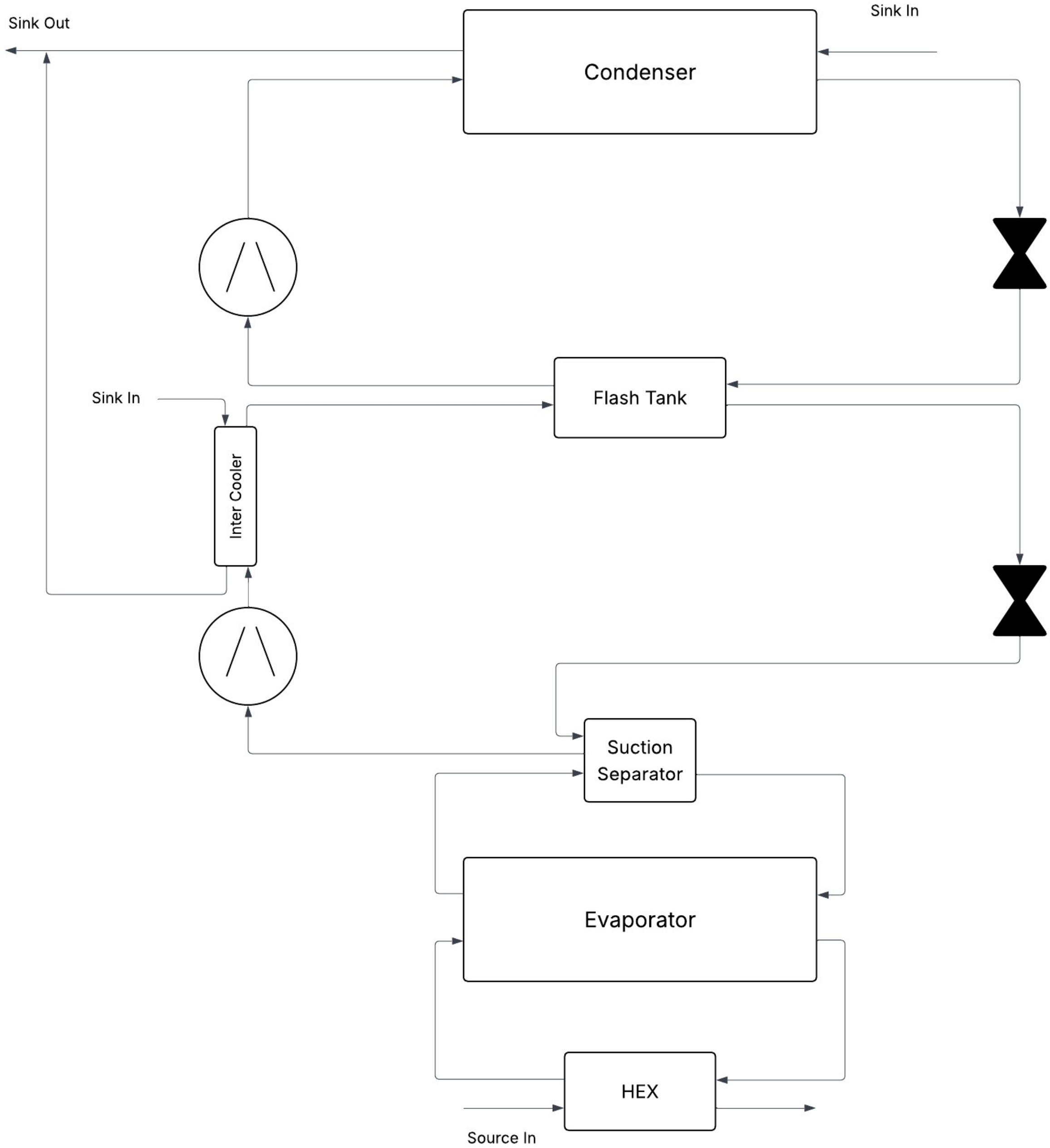

Figure 5: System sketch of the two-stage ammonia cycle.

4.2 Two-Stage Cascade Cycle

The system is modelled as a two-stage cascade configuration, utilizing two refrigerants to optimize performance across a wide temperature lift. The low-temperature cycle employs propane, which interacts with the heat source via an intermediate fluid loop and an external heat exchanger. Because propane is highly flammable, this configuration serves as a critical safety barrier that minimizes the refrigerant charge. The high-temperature cycle, on the other hand, utilizes isobutane. This specific arrangement of the refrigerants within the cascade cycle is governed by two primary thermodynamic constraints. Firstly, isobutane is unsuited for the low-temperature stage due to its low pressure at decreased temperatures. At evaporating temperatures around -10 °C, the saturation pressure of isobutane approaches sub-atmospheric levels. Operating under vacuum conditions poses a significant risk of air and moisture ingress into the system, which compromises safety and efficiency, while also severely limiting the acceptable temperature range of the heat source.

Secondly, placing propane in the high-temperature upper stage is avoided due to its relatively low critical temperature (approximately 96.7 °C). To meet the highest supply temperatures demanded by the district heating network, an upper-stage propane cycle would be forced into transcritical operation. Furthermore, the core of this architecture is the cascade heat exchanger (see Figure 6), which functions as a thermal link where the heat rejected by propane is directly recovered as the evaporative heat source for the isobutane circuit.

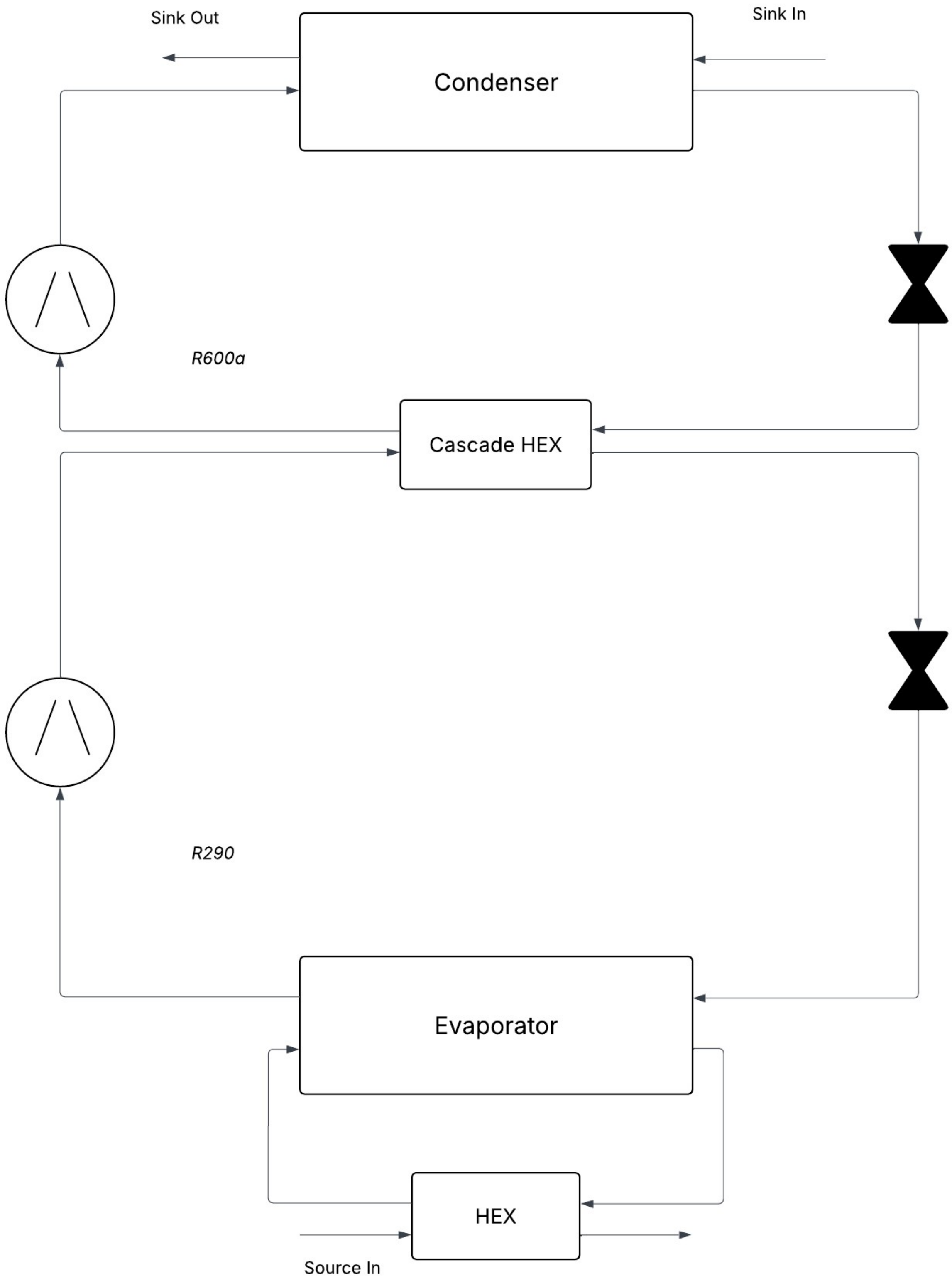

Figure 6: System sketch of the two-stage hydrocarbon cascade cycle.

4.3 One-Stage Transcritical Ejector Cycle

The carbon dioxide system is modelled as a transcritical cycle integrated with an ejector to recover expansion work. Due to the low critical temperature of carbon dioxide, heat rejection occurs in a gas cooler where the refrigerant remains in a supercritical state, allowing for a gliding temperature match with the DH sink. A central component of this specific model is the ejector, which replaces the traditional expansion valve as the primary expansion device (see Figure 7). The ejector utilizes the high-pressure energy from the gas cooler to entrain and compress the vapor from the evaporator, raising the suction pressure.

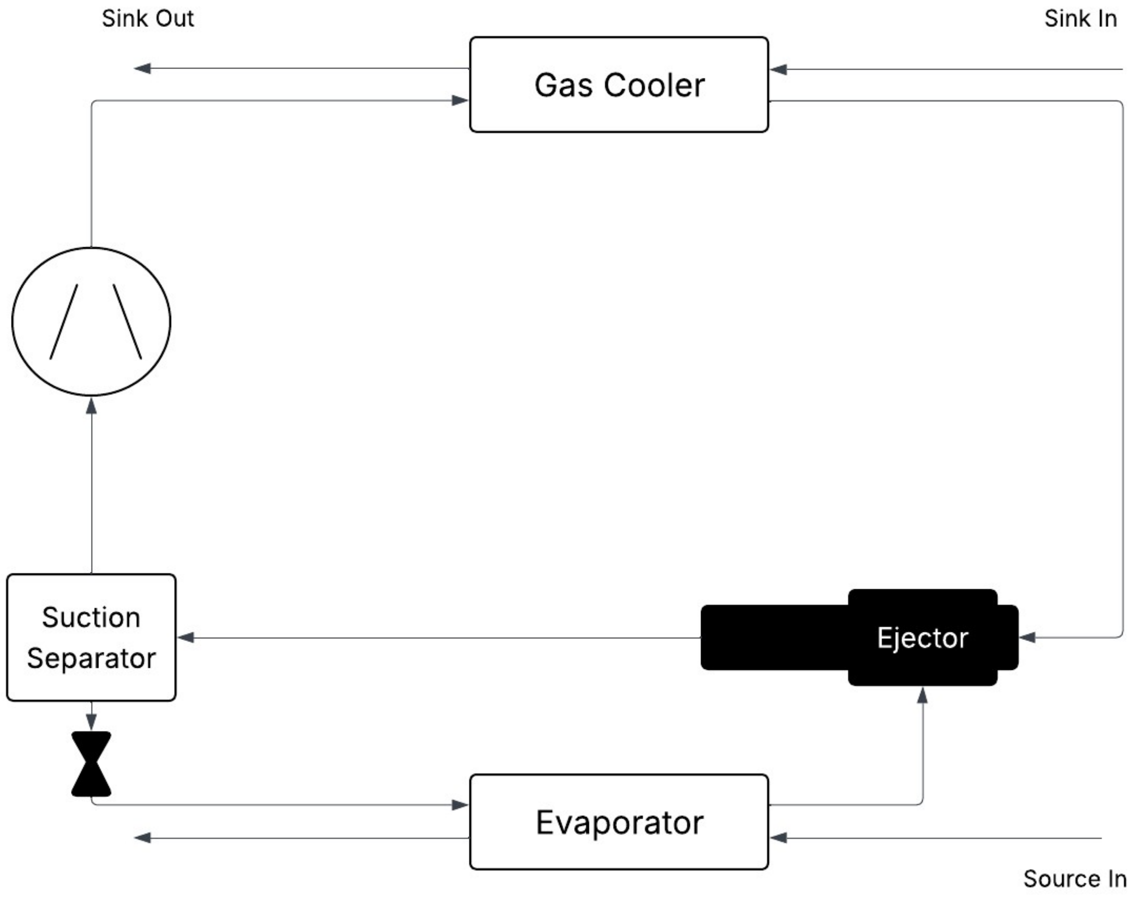

Figure 7: System sketch of the transcritical carbon dioxide cycle.

4.4 Thermodynamic Modelling

The performances of the heat pump systems are evaluated using a deterministic modelling approach, where the state of the refrigerant is calculated at each discrete point in the cycle. The model is developed in Python, utilizing the CoolProp open-source library for thermophysical fluid properties.

4.4.1 Suction State Determination

To establish the baseline for the compression process, the evaporation pressure (P_{evap}) is determined by the saturation temperature required to facilitate heat transfer from the source. This is calculated accordingly with the expression in Equation 3:

$$T_{sat,evap} = T_{source} - \Delta T_{approach} - \Delta T_{superheat} \quad (3)$$

where $\Delta T_{approach}$ represents the approach temperature difference in either evaporator or evaporator plus external heat exchanger, depending on the occurrence of a secondary loop, and $\Delta T_{superheat}$ represents the fixed degree of internal superheating in the evaporator. In any system fitted with a separator or a flash tank (or both), the refrigerant is considered as saturated vapour after that component.

4.4.2 Pinch Point Analysis

The determination of the discharge pressure is a critical step in the modelling process, as it directly influences both the heat capacity and the compressor work. Due to the different phase behaviours of the selected refrigerants, two distinct iterative methodologies are employed to ensure that the second law of thermodynamics is satisfied via a minimum pinch point temperature difference (ΔT_{pinch}).

Subcritical Heat Rejection (R717 and hydrocarbon cascade):

For the subcritical cycles, the heat rejection process is characterized by desuperheating, condensation at a constant temperature, and subcooling. The model assumes that the pinch point, the location of the minimum temperature difference between the refrigerant and the sink, occurs at the onset of condensation (the saturated vapour point). To determine the correct condensing pressure, the model performs a localized energy balance. For a given trial pressure, the refrigerant's enthalpy at the saturation point is identified. The corresponding temperature of the district heating water at this specific point is then calculated by evaluating the energy balance between water temperature increment and refrigerant enthalpy decrement. The iteration process continues, using a numerical solver, until the temperature difference at this junction matches the predefined pinch point difference. Once convergence is reached, the condensing pressure is established.

Transcritical Heat Rejection (R744):

In the transcritical cycle, the heat rejection occurs in the supercritical region where the refrigerant does not undergo a constant-temperature phase change. Instead, it exhibits a non-linear temperature glide in the gas cooler. Since the specific heat capacity of carbon dioxide varies significantly near the pseudo-critical line, the location of the pinch point is not fixed and can shift depending on the operating pressure. To account for this, the gas cooler process is discretized into a high-resolution enthalpy grid. For each trial pressure, the refrigerant temperature is calculated at every step. Simultaneously, the corresponding sink temperature is derived through a cumulative energy balance along the heat exchanger. The model monitors the temperature difference throughout the entire glide accordingly with Equation 4:

$$\Delta T(h) = T_{refrigerant}(h, P) - T_{sink}(h) \geq \Delta T_{pinch} \tag{4}$$

A range of permissible pressures that satisfy the pinch point constraint across the entire heat exchanger is evaluated. From this set, the model selects the pressure that optimizes the system's COP, thereby simulating a high-level gas cooler pressure control strategy.

4.4.3 Compressor Performance Modelling

To ensure that the model accurately reflects the performance of industrial-scale equipment, the compressor efficiencies were not treated as constants. Instead, they were derived through regression analysis based on empirical data obtained from a major manufacturer's selection software. Data for mass flow rate and electrical power input were collected across a wide range of operating envelopes, covering various combinations of evaporation and condensation temperatures (and gas cooler pressures for the transcritical system). Using CoolProp, these data points were processed to calculate the volumetric efficiency and the overall isentropic efficiency for each operating point.

To generalize these efficiencies for the hourly simulation, each data point was mapped to its corresponding pressure ratio $\Pi = P_1/P_2$. The relationship between efficiency and pressure ratio was then established using numerical regression techniques in NumPy, allowing for extrapolation outside of the manufacturer's stated operational envelope:

- **Overall Isentropic Efficiency:** The isentropic efficiency, which in this context accounts for all internal losses (thermodynamic, mechanical, and internal electrical losses), was modelled using a second-order polynomial regression with the form given in Equation 5:

$$\eta_{is,tot} = a\Pi^2 + b\Pi + c \tag{5}$$

- **Volumetric Efficiency:** The volumetric efficiency, which dictates the actual volumetric flow rate relative to the compressor's swept volume, was found to best follow a linear relationship with the form given in Equation 6:

$$\eta_{vol} = kx + m \tag{6}$$

4.4.4 Assumptions and Constraints

Table 2 summarizes the assumptions made regarding the thermodynamic cycles, along with constraints in operational envelope. They have been established based on manufacturer data for relevant compressors as well as discussion with supervisors.

Table 2: Thermodynamic assumptions.

Parameter	Symbol	Value	Unit
Approach Temperature Difference at External HEX	$\Delta T_{approach}$	3	K
Approach Temperature Difference at Evaporator	$\Delta T_{approach}$	3	K
Approach Temperature Difference at Condenser/Gas Cooler	$\Delta T_{approach}$	7	K
Approach Temperature Difference at Inter Cooler	$\Delta T_{approach}$	5	K
Ejector Efficiency	η_{ej}	30	%
Internal Superheating Evaporator	$\Delta T_{superheat}$	5	K
Pinch Point Temperature Difference	ΔT_{pinch}	3	K

4.5 Operational Logic

The operational strategy of the heat pump system is governed by an hourly logic designed to minimize the operational heat production cost of the district heating (DH) system. The model evaluates whether the heat pump should operate based on real-time market data, technical constraints, and DH network requirements.

4.5.1 Dispatch Decision

The fundamental decision-making process is based on an operational cost comparison between the heat pump and the existing biomass-based heat production. At each hour *t*, the model evaluates which unit represents the least-cost option for satisfying the DH demand. The operational cost of heat produced by the heat pump (OC_{hp}) is composed of the electricity spot price, grid-related variable costs, and electricity tax. This study accounts for the full variable cost per energy unit of heat produced accordingly with Equation 7:

$$OC_{hp,t} = \frac{C_{spot,t} + C_{trans} + C_{tax}}{COP_t} \tag{7}$$

Where:

- $C_{spot,t}$ is the hourly electricity spot price [SEK/MWh].
- C_{trans} represents the variable transmission fee (energy compensation) for the electricity grid [SEK/MWh].
- C_{tax} is the national energy tax on electricity [SEK/MWh].
- COP_t is the instantaneous coefficient of performance.

The reference operational cost for the biomass boiler (OC_{bio}) is calculated based on the fuel price and the unit's efficiency. In accordance with Swedish tax legislation, bio-based fuels are exempt from both carbon and energy taxes, meaning the operational cost is driven by fuel procurement.

$$OC_{bio} = \frac{C_{biomass}}{\eta_{boiler}} \tag{8}$$

Where:

- $C_{biomass}$ is the cost of the biomass fuel [SEK/MWh_{heat}].
- η_{boiler} is the energy efficiency of the boiler, assumed to be equal to 85%.

The heat pump is prioritized in the dispatch only when the operational cost of it is lower than that of biofuel-based heating. This comparison ensures that the model captures the impact of electricity taxes and transmission fees, which reduce the economic room for heat pump operation even when spot prices are low. When the heat pump cannot meet the entire heating demand, the biofuel boiler provides the remaining part as visualised on the left-hand side of Figure 8. Regardless of the heat pump being aimed to operate or not, its available capacity in terms of electricity consumption at each time step is used to bid with on the mFRR market. It should, however, be noticed that the boiler cannot perfectly regulate its capacity at lower load. The minimum capacity possible to run the boiler at has been assumed to be 15 MW, meaning that the boiler must be prioritized regardless of operational cost when the difference between heat pump heating capacity and demand is less than that value.

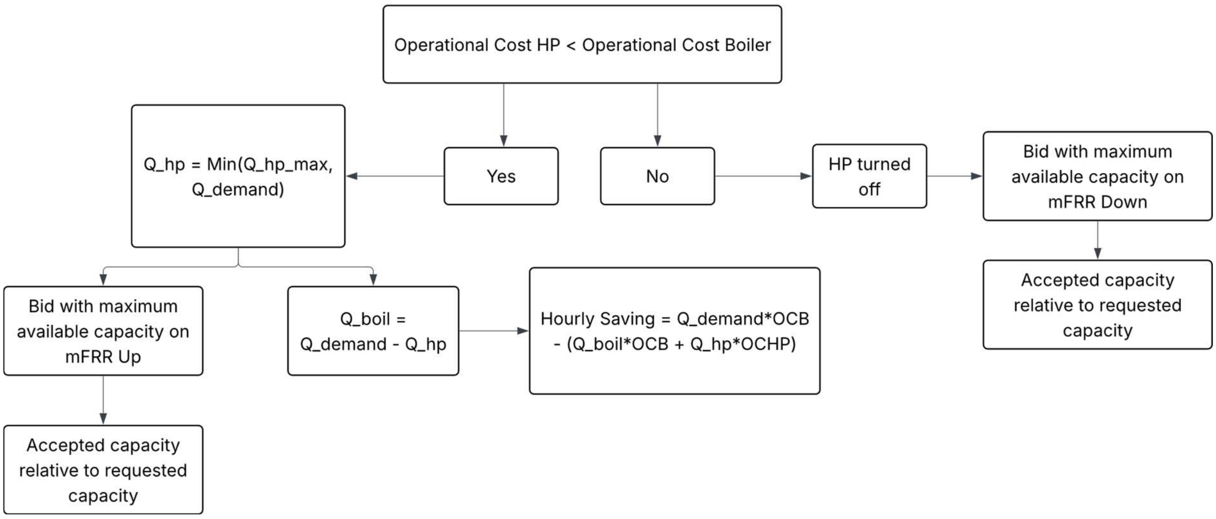

Figure 8: Flowchart of the operational logic.

4.5.2 Capacity Regulation and Grid Constraints

To ensure the model reflects a realistic integration into the existing energy infrastructure, two primary technical constraints are applied to the heat pump's hourly heating capacity at full compressor speed:

1. **Thermodynamic Maximum:** The maximum heating capacity determined by the compressor's swept volume and current operating pressures.
2. **Grid Demand Limitation:** The heat pump is constrained by the actual hourly heat demand of the DH network. If the maximum possible heat output exceeds the instantaneous demand, the system is modelled to modulate its capacity (via frequency control), reducing the output such that heating capacity is equal to demand.

The electrical power consumption is subsequently adjusted based on the part-load output, assuming a constant COP for the specific hourly temperature setpoints.

4.5.3 Balancing Market Integration (mFRR)

Beyond substitution of fuel, the heat pump system is modelled as a flexible resource on the mFRR market. The integration logic is based on the principle of offering capacity that deviates from the unit's planned operation. The direction of the capacity bid depends on the initial dispatch decision derived from the operational cost comparison. If the heat pump is scheduled to operate, it can offer downward regulation (decreasing heat output). Conversely, if the unit is scheduled to be idle, it can offer upward regulation (increasing heat output). This dual capability allows the system to provide grid services regardless of the initial dispatch decision.

To reflect the practical limitations of participating in a competitive balancing market, several stochastic and technical factors were integrated:

- **Bidding Efficiency:** Since mFRR bids in practice must be submitted ahead of time, a bidding efficiency factor was applied. This factor accounts for the forecasting errors associated with predicting heat demand and available capacity one day in advance, preventing the model from achieving perfect foresight. In the model, 90% of the possible bidding capacity is bided with in each time step. The number used has no statistical basis and has rather been chosen arbitrarily based on the typical accuracy of weather forecasts for the next 24 hours.

- **Acceptance Probability:** The greater the demand (requested volume), the greater the likelihood that the bids will be accepted. Thus, the model weights the probability for acceptance against the relation between requested capacity and the heat pump's bidding capacity. With the heat pump's market share being equal to or less than 10%, it's assumed that the bid is very likely (98% certainty) to be accepted. When the market share is more than 50%, it's assumed that the bid is unlikely (20% certainty) to be accepted. A sliding scale is used in between.
- **Market Share Limitation:** To account for market liquidity and competition, the accepted bid capacity is considered never to be more than 25% of the total market demand for mFRR at each specific hour. This ensures that the model does not assume unrealistically large market penetrations.
- **Weighted Activation Penalty:** The economic impact of an activation is modelled as the product of the hourly opportunity cost and the probability of activation. The opportunity cost represents the financial loss of deviating from the optimal energy dispatch (e.g., forced operation during high-price hours or forced idling when heat pump production is cheaper than biomass). This hourly penalty is weighted against a stochastic activation probability derived from historical market data, in accordance with Equation 9:

$$C_{activation,t} = \left(MC_{hp,t} - MC_{bio,t}\right) \cdot P(activation)_t \tag{9}$$

- **Aggregator Fee:** A 20% service fee is deducted from the gross balancing revenue to account for the participation costs through a third-party aggregator.

This approach ensures that the balancing revenue is not merely a theoretical maximum, but a risk-adjusted estimate that considers market dynamics, forecasting limitations, and the true cost of operational deviations.

4.5.4 Grid Tariff Structure and Net Savings

The economic evaluation aggregates all operational revenues and costs to determine the project's viability. A significant component of the total operational expenditure of the heat pump is the electricity power tariff, which is modelled in accordance with a specific power demand charge structure inspired by one of the distribution system operators (DSO). It is important to note that the grid capacity charge is not included in the hourly dispatch logic described in section 4.3.1. Due to the complexity of predicting the monthly power peaks in a real-time environment, the model assumes that the heat pump is operated solely based on marginal energy costs. The power demand charges are instead calculated ex-post, once the consumption pattern for each month is fully mapped. The billable power is calculated based on a monthly average of the three highest hourly power peaks, provided that these peaks occur on different calendar days. Furthermore, it is divided into two separate charges:

- Regular monthly charge: Applied for every month, regardless of consumption pattern.

- Peak period charge: Applied for usage between 6 am and 10 pm during November, December, January, February, and March.

The total monthly charge is derived by taking the arithmetic mean of the three highest recorded values from separate days and multiplying this average by the capacity fee. The total annual net saving (S_{total}) summarizes the economic impact of partially substituting biofuel with heat pump in the heat production while accounting for the flexibility revenues and the additional grid capacity costs. The performance metric is defined as the expression in Equation 10:

$$S_{total} = \sum_{t=1}^{8760} (Marginal\_Savings_t + mFRR\_Revenue_t) - \sum_{m=1}^{12} Cost_{grid,m} \quad (10)$$

4.5.5 Net Present Value and Investment Potential

To evaluate the economic feasibility of the different heat pump systems, the net present value (NPV) method is utilized. It is used to determine the justified capital expenditure (CAPEX), which is defined as the investment cost that results in an NPV of zero, given a specific discount rate and economic lifespan. Using the total annual net saving (see 4.3.4), the justified CAPEX is derived from the following formula:

$$Justified\ CAPEX = \sum_{t=1}^{n} \frac{S_{total}}{(1+r)^t} \quad (11)$$

Where:

- S_{total} is the total net annual saving [SEK/year].
- *r* is the real discount rate [%].
- *n* is the economic lifespan of the investment [years].
- *t* is the specific year of the cash flow.

Table 3: Economic assumptions.

Parameter	Value	Unit
Discount Rate	5	%
Expected Lifespan	15	yrs.

The model assumes that the annual net savings remain constant in real terms throughout the investment period. By employing a real discount rate, the impact of general inflation is inherently accounted for, as both future energy prices and the discount rate are expressed in the same currency value. This approach provides a clear threshold for the total project cost including equipment, installation, and grid connection above which the investment would no longer meet the required rate of return.

5 Case Study and Input Data

This chapter presents the boundary conditions and input data used for the simulations. The data used represents a full operational year to capture seasonal variations in heating demand, ambient temperatures, and energy prices.

5.1 Large-scale Urban Network

The studied case is a district heating system situated in a city with a population of approximately 40,000 inhabitants. The network is located in electricity bidding zone SE4, a region characterized by high electricity price volatility and a close connection to the continental European power grid.

- **Heating Demand:** The system has an annual heating demand of approximately 375 GWh.
- **Existing Production:** The reference production unit is a centrally located biomass boiler (wood chips).
- **Sizing Strategy:** Following the requirements from the local district heating utility during a feasibility study conducted by EKA, the heat pump is dimensioned to meet the heating demand during the summer season (low-load period).
- **Design Point:** The heat pump system is sized to deliver 15 MW of heating at a representative summer design point, defined as:
    - **Source Temperature:** 15 °C (ambient air).
    - **Sink Temperatures:** 55 °C return and 80 °C supply.

5.2 Network Temperature Profiles

The simulation utilizes hourly historical data for supply and return temperatures to ensure that the heat pump's performance is evaluated against realistic operational conditions. This data-driven approach captures the actual dynamics of the district heating network, which are influenced by consumer behaviour and seasonal weather patterns. Figure 9 illustrates the relationship between the ambient outdoor temperature and the network temperatures. The data shows a clear correlation where supply temperatures increase as the outdoor temperature drops, while return temperature exhibits a non-linear U-shaped tendency. The supply temperature varies between approximately 80 °C and 110 °C, while the return temperature fluctuates between 40 °C and 60 °C. Supply and return temperature data is sourced from EKA.

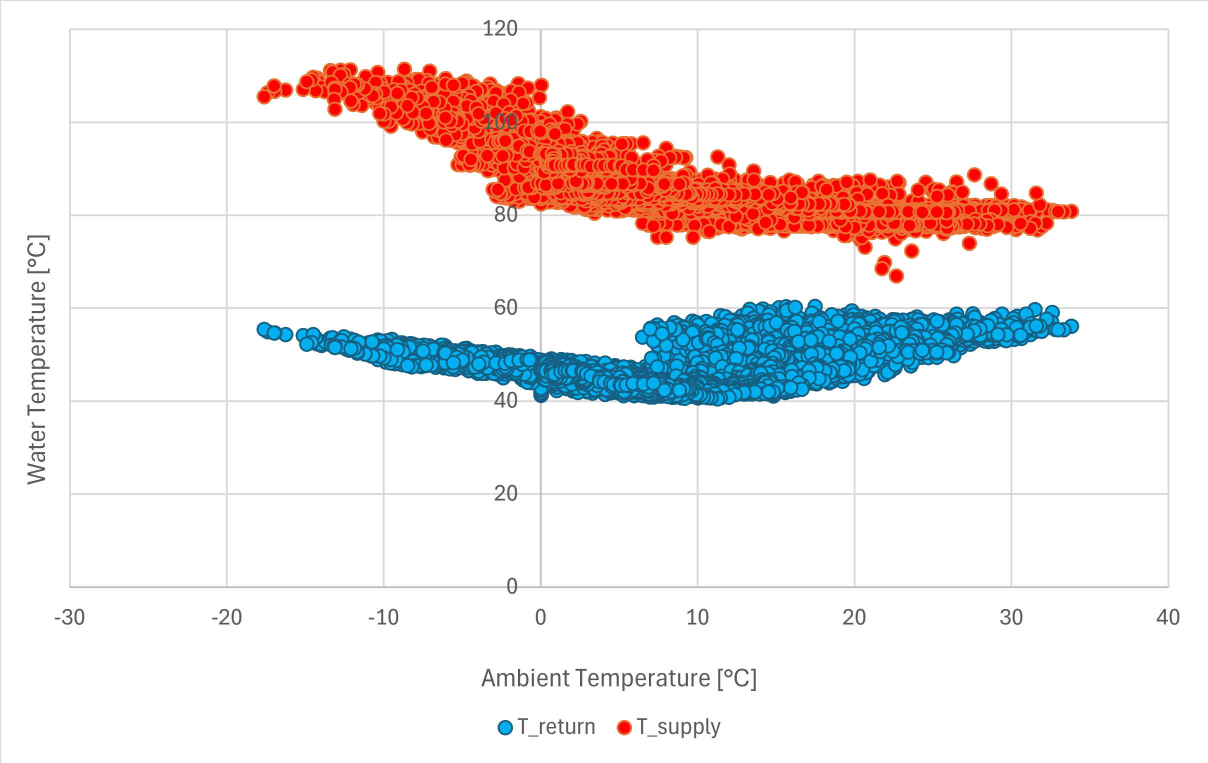

Figure 9: Supply and return temperature fluctuations relative to ambient temperature.

5.3 Heat Source Characteristics

The investigated system utilizes ambient air as heat source. Data shows a temperature range spanning from approximately -20 °C to 35 °C (see Figure 9). However, as illustrated in the duration curve in Figure 10, the majority of the operating hours occur within a smaller temperate range. The figure shows that for approximately 7,500 hours of the year, the ambient temperature remains above 0 °C, which indicates that the heat pump operates under relatively favourable conditions for most of its annual production. Ambient air temperature data is sourced from EKA.

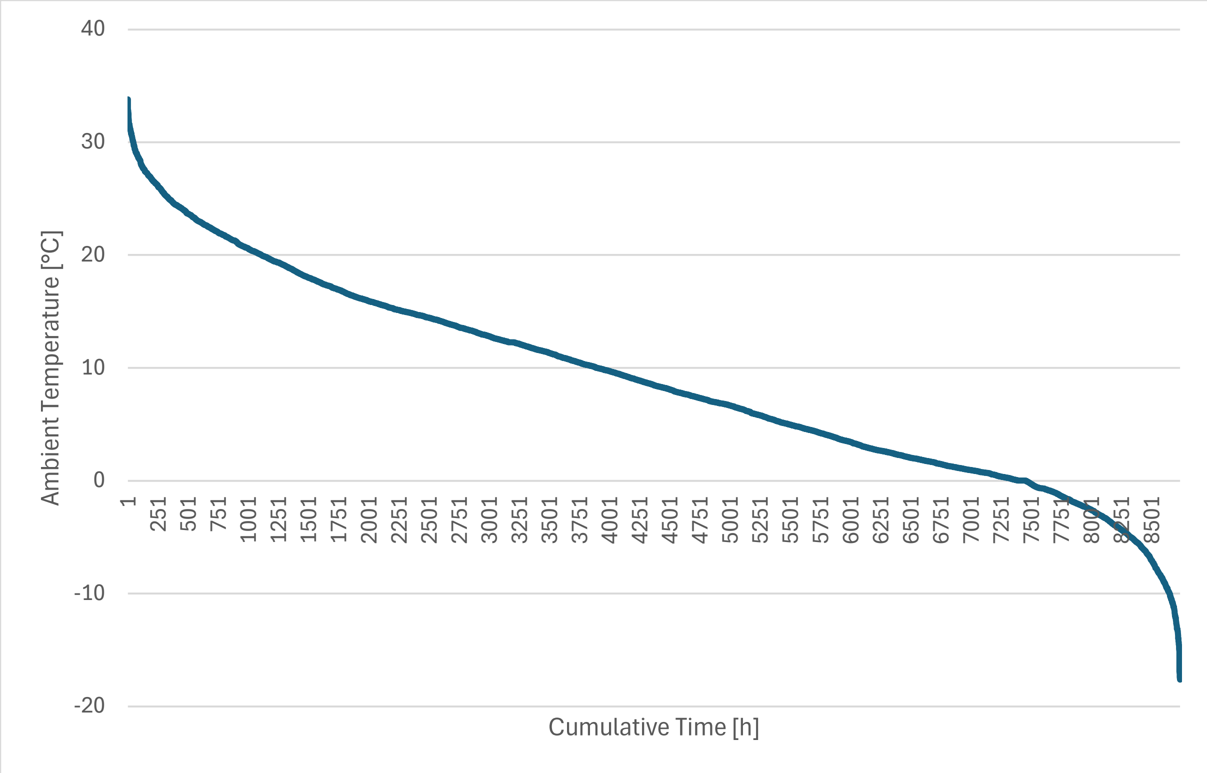

Figure 10: Ambient temperature duration curve.

5.4 Load Profile

The total annual heating demand is approximately 375 GWh. To accurately simulate the heat pump's possible contribution, hourly load data was used as an input. This allows the model to determine the share of the load covered by the heat pump versus the existing biomass boiler at any given time. As illustrated in Figure 11, the heating demand during the studied year reached its minimum during the period from June to August, stabilizing at an average load of approximately 8 MW. Heating demand data is sourced from EKA.

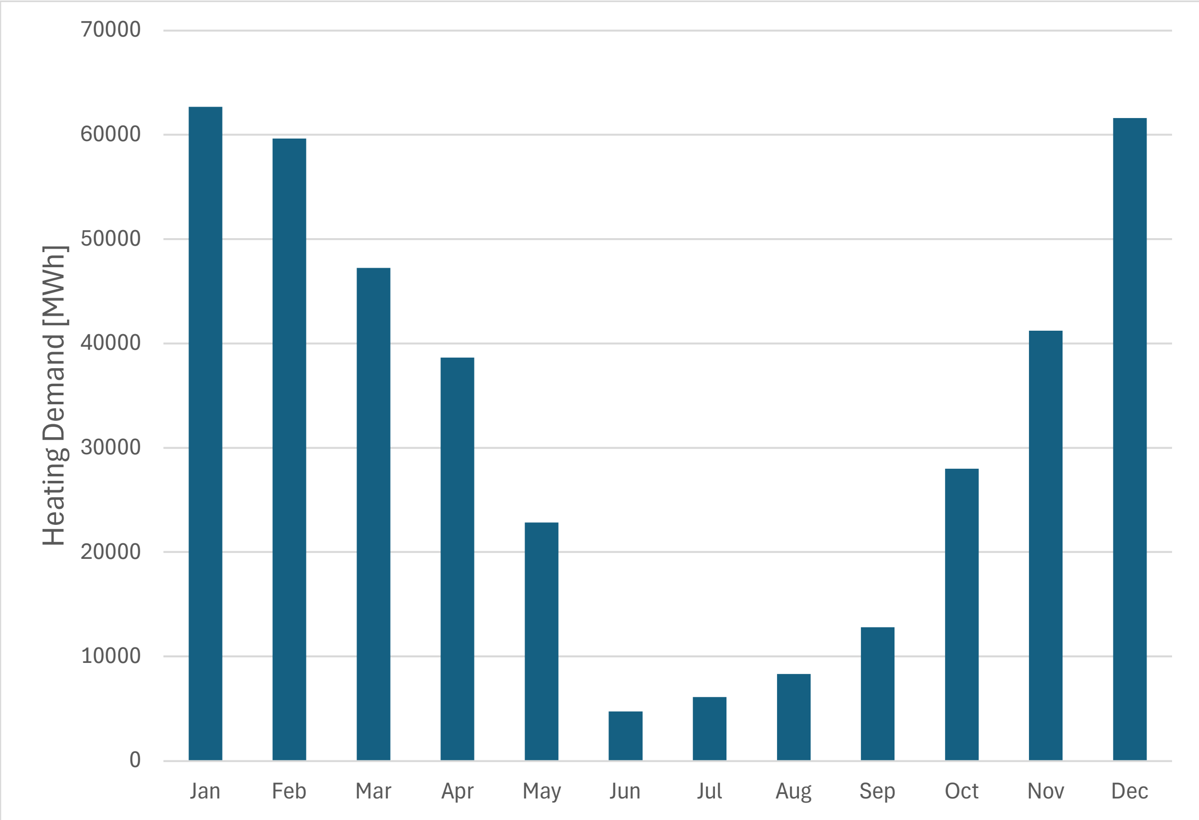

Figure 11: Monthly heating demand profile over the calendar year used.

5.5 Electricity Spot Prices

The economic performance of the simulated heat pump is driven by the hourly electricity spot prices in bidding zone SE4. Figure 12 presents the price duration curve for the simulated year in that region. The curve illustrates a market characterized by high price variance, which is a critical factor for the operational logic of the heat pump. The left side of the curve shows extreme price peaks, reaching levels above 500 öre/kWh, while the right tail of the curve highlights periods of very low or even negative electricity prices. For the most part (approximately 4,500 hours), the price remains between 50 and 150 öre/kWh. This range defines the normal operating conditions where the heat pump's COP becomes the deciding factor for its competitiveness. Spot price data is sourced from ENTSO-e.

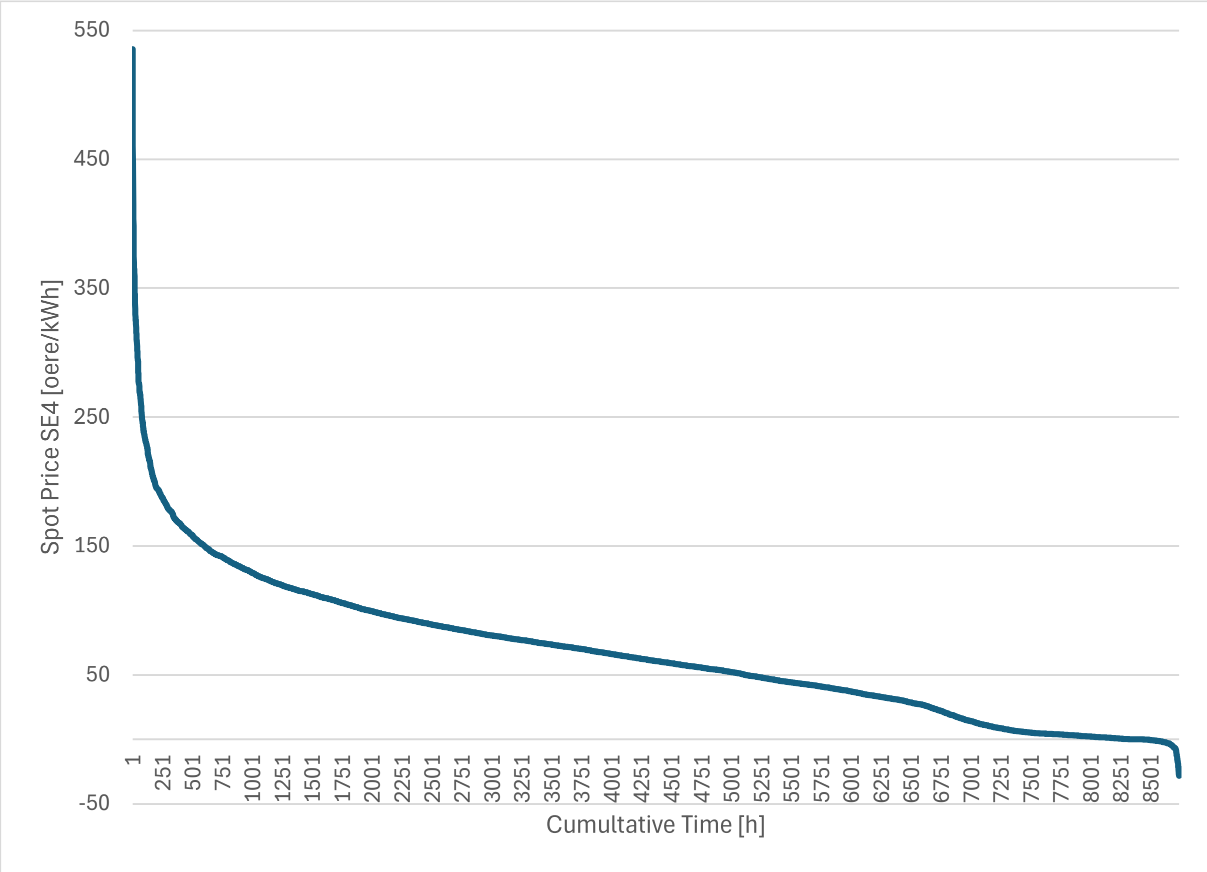

Figure 12: Price duration curve for SE4 in 2025.

5.6 Biomass and Auxiliary Fuel Costs

The biofuel price used in the model is represented by the average wood chip price across Sweden. Data is sourced from the Swedish Energy Agency.

Table 4: Average wood chip prices in Sweden in 2025, quarterly.

	Biofuel Price	
Q1	383	SEK/MWh
Q2	387	SEK/MWh
Q3	372	SEK/MWh
Q4	363	SEK/MWh

5.7 Grid Tariffs and Taxes

Beyond the electricity spot price, grid related tariffs and taxes must be included to yield the overall price for electricity use. For this study, the pricing model for Vattenfall's N2T high-voltage supply contract is used, and the actual numbers used are for year 2025. Minor changes regarding the definition of peak period are done relative to Vattenfall's model, due to simulation simplicity.

Table 5: Grid tariffs and electricity tax used in the model. Design inspired by Vattenfall's N2T contract, and numbers valid for 2025.

Grid Charge		
Fixed Fee	28 500	SEK/month
Power Fee Regular***	34	SEK/kW, month
Power Fee Peak*	49	SEK/kW, month
Transmission Fee Regular**	6.4	öre/kWh
Transmission Fee Peak*	12.2	öre/kWh
Electricity Tax	43.9	öre/kWh

*Peak period defined as 6 am-10 pm during January, February, March, November and December.
**Outside of peak period.
***Every month of the year.

5.8 Balancing Market Data (mFRR)

The collected data for the manual frequency restoration reserve reveals a market environment characterized by significant volatility and distinct seasonal shifts, which directly reflects the complexities of balancing the Swedish power grid. When examining the relationship between capacity price (see Figure 13) and procured volume (see Figure 14), a clear trend emerges where the market's liquidity increases steadily throughout the year. This expansion in procured volume generally leads to more stable capacity pricing, though specific periods, most notably in March and June, exhibit sharp increases in both price levels and statistical dispersion. These spikes, visible as elongated boxes and whiskers in the capacity price plot, suggest intervals of reduced system margins where the cost of securing availability rises significantly due to tightening supply or increased grid stress. Balancing market data is sourced from the Mimer platform (Svenska kraftnät).

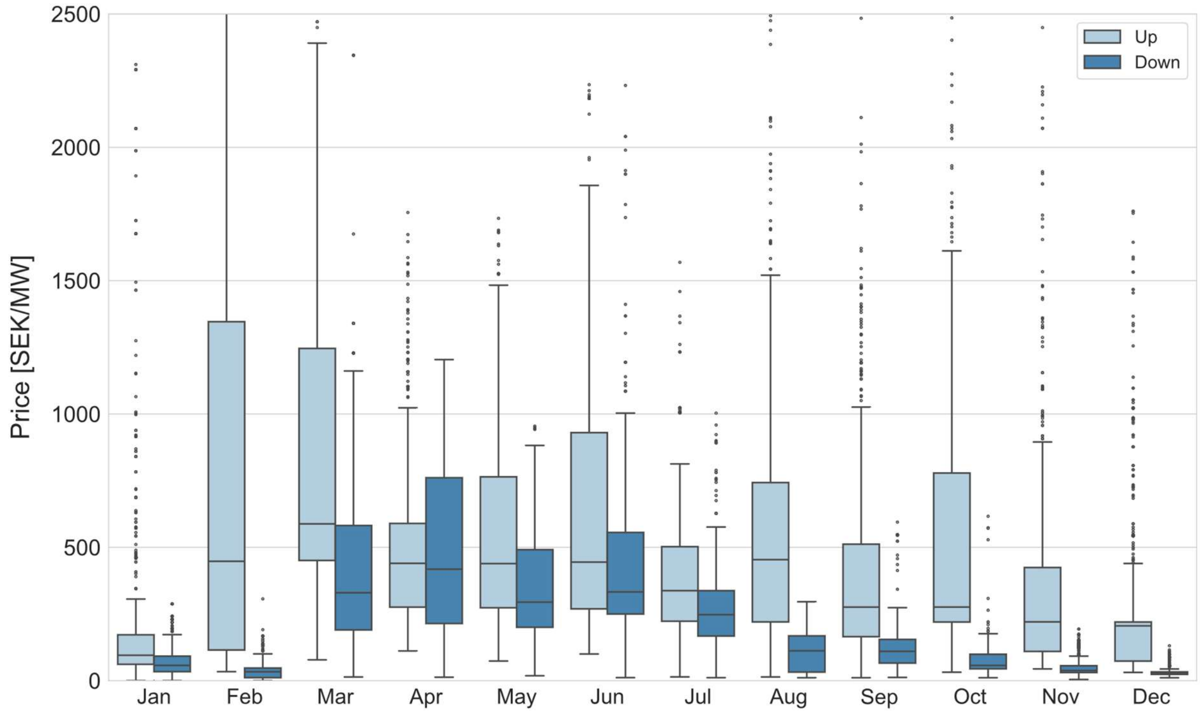

Figure 13: Capacity prices for 2025 in zone SE4. Boxes show interquartile ranges and medians.

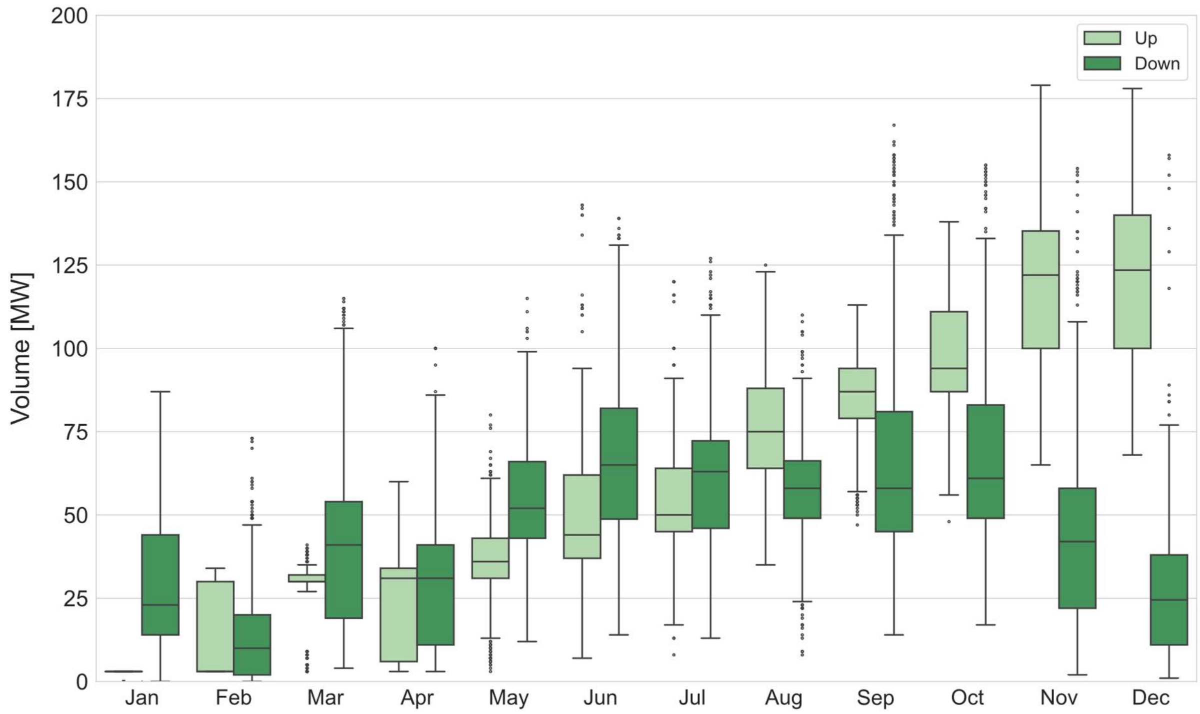

Figure 14: Procured capacity volume for 2025 in zone SE4. Boxes show interquartile ranges and medians.

6 Results

The simulation results regarding technical performance and economic feasibility are presented and described in this section.

6.1 COP Sensitivity

This section presents the thermodynamic performances of the investigated configurations. COP is determined as a function of the heat source temperature across different district heating temperature regimes. The relationship between COP and the heat source temperature is visualized for three distinct operational cases, representing varying return and supply temperatures within a typical district heating network (see Figures 15, 16, and 17).

- **Low-temperature regime (T_{ret} = 35 °C, T_{sup} = 75 °C):** At these temperature conditions, the ammonia configuration is the top-performing system across the entire source temperature range, demonstrating a stable and near linear increase in COP. The cascade system maintains a clear advantage over the transcritical carbon dioxide cycle at lower and intermediate source temperatures. However, due to a flattening performance trend for the cascade system, a crossover occurs at approximately 12 °C where the cascade configuration underperforms compared to carbon dioxide.

- **Intermediate-temperature regime (T_{ret} = 43 °C, T_{sup} = 85 °C):** As the temperature lift increases, a general reduction in COP is observed for all configurations. At the source temperature of approximately -8 °C, the cascade system achieves an efficiency identical to the ammonia system, which otherwise remains the top-performing configuration across the remaining interval. While the cascade system exhibits a flattening performance trend at higher source temperatures, it maintains a clear advantage over the transcritical carbon dioxide cycle across the entire investigated range.

- **High-temperature regime (T_{ret} = 51 °C, T_{sup} = 90 °C):** At the highest investigated temperature lift, the ammonia configuration remains the top-performing system overall. However, the cascade system demonstrates a strong performance, closely matching and shifting to tangent the ammonia curve over a relatively wide intermediate section of the source temperature interval. At the upper end of the range, the cascade performance flattens out against ammonia, while the transcritical carbon dioxide cycle consistently performs worse and remains well below both configurations across the entire spectrum.

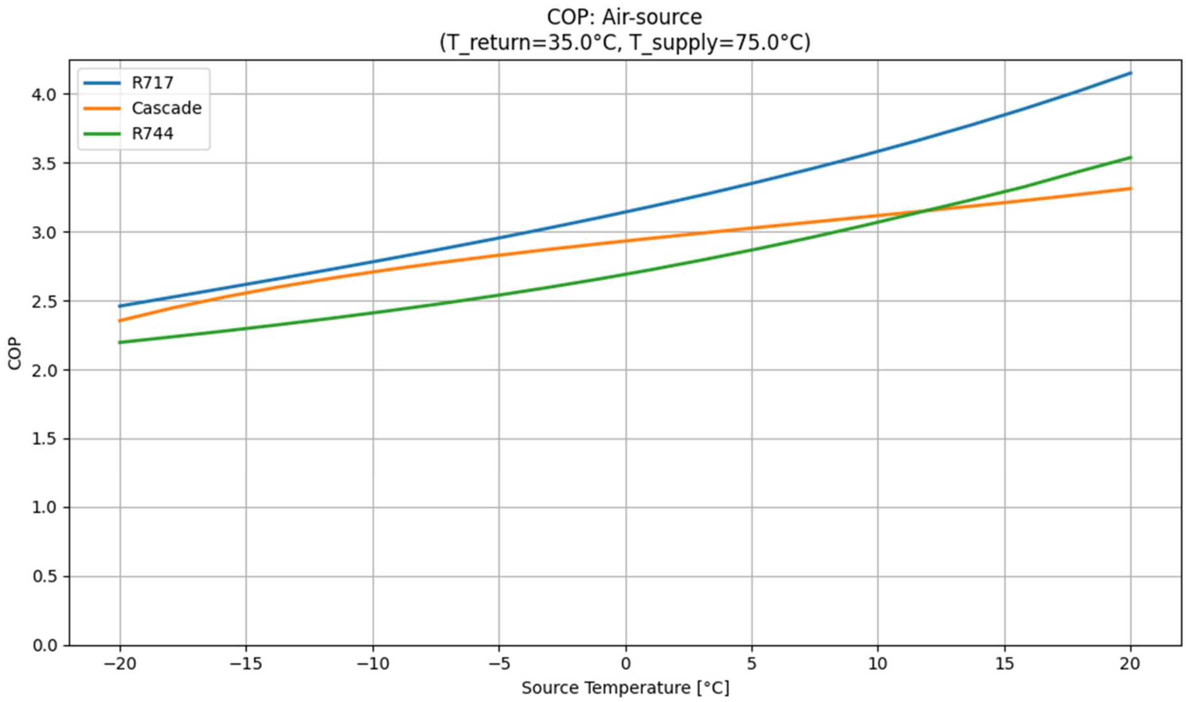

Figure 15: COP as a function of source temperature at T_{ret} = 35 °C and T_{sup} = 75 °C.

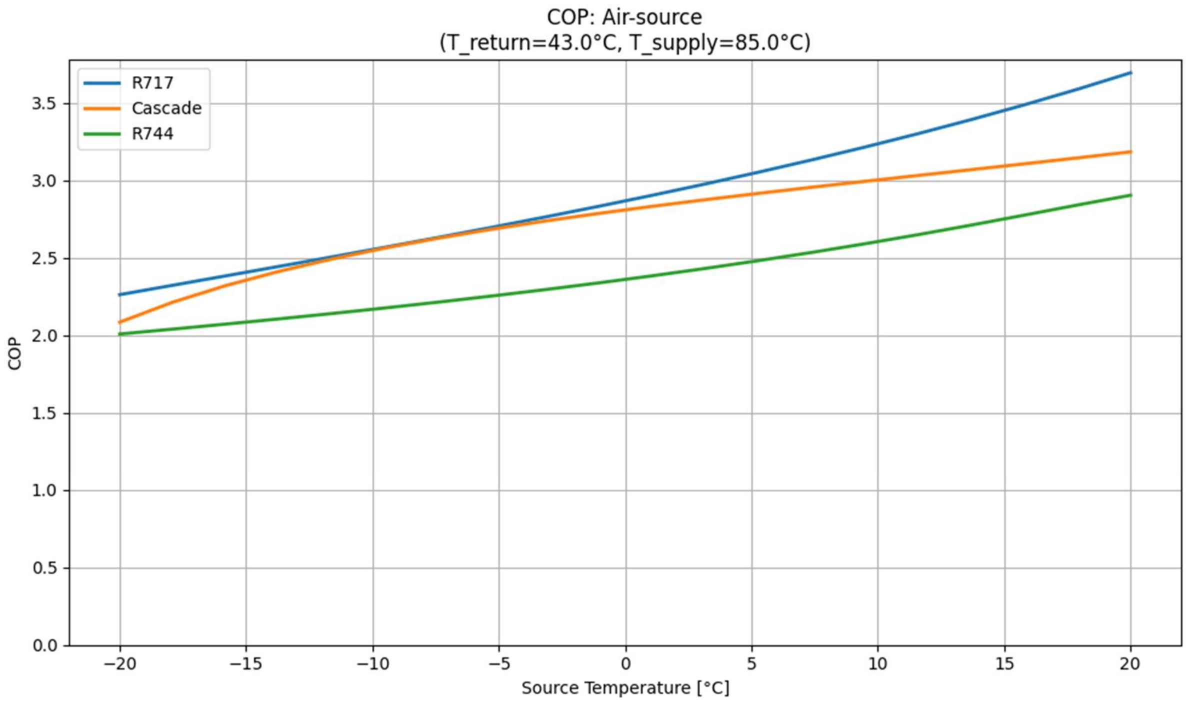

Figure 16: COP as a function of source temperature at T_{ret} = 43 °C and T_{sup} = 85 °C.

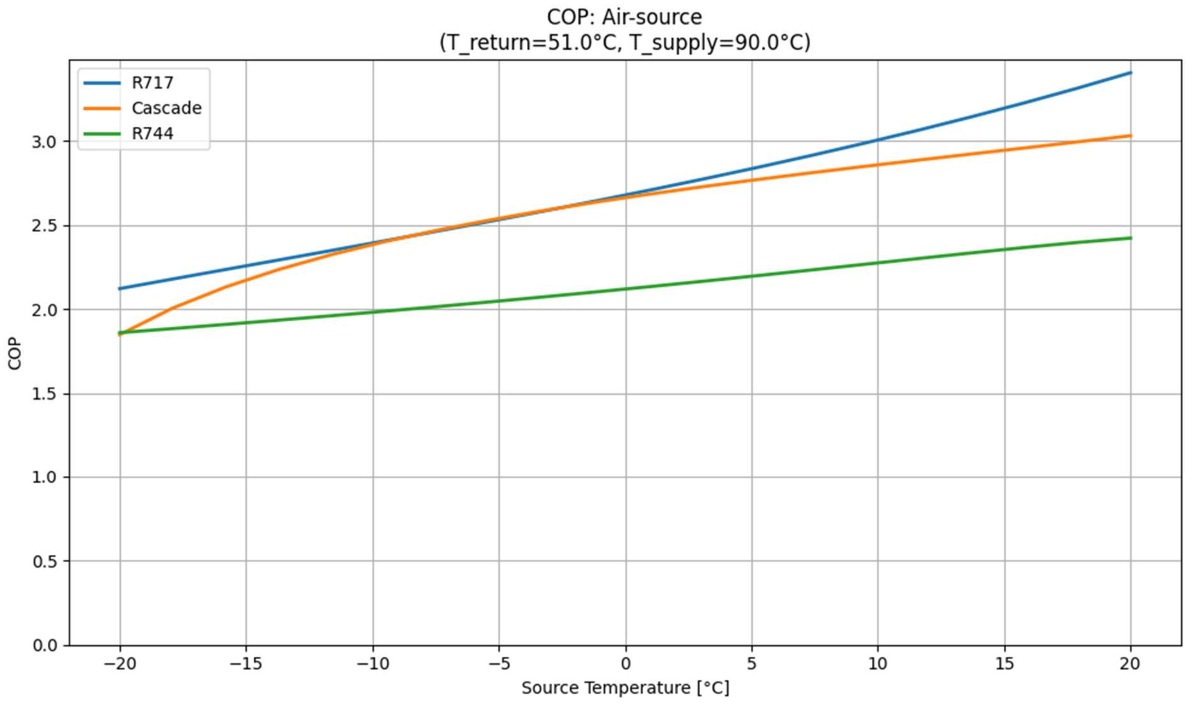

Figure 17: COP as a function of source temperature at T_{ret} = 51 °C and T_{sup} = 90 °C.

6.2 Economic Outcomes

This section presents the financial results derived from the simulations of ammonia, hydrocarbon cascade, and carbon dioxide under the defined case study conditions. The results include annual savings, grid-related costs, and the calculated justified CAPEX.

6.2.1 Annual Savings and Operational Data

The economic performance is compiled based on energy cost displacement and revenues from the mFRR market. Table 6 summarizes the key financial and operational metrics for the investigated systems. The results demonstrate a financial advantage for the two-stage ammonia system, which achieves the highest total annual savings of 17.5 MSEK. The cascade system containing hydrocarbons performs slightly worse, with similar marginal savings but significantly higher grid power costs. Carbon dioxide performs the lowest net savings, less than half of the net savings for both other configurations.

Table 6: Economic and technical results.

Metric	Ammonia (R717)	Cascade (R290 & R600a)	Carbon Dioxide (R744)	Unit
Marginal Savings	15.68	14.85	7.84	MSEK/year
mFRR Net Revenue	4.77	5.48	4.01	MSEK/year
Grid Power Cost	2.95	4.07	4.29	MSEK/year
Grid Fixed Cost	0.342	0.342	0.342	MSEK/year
Total Net Savings	17.16	15.91	7.23	MSEK/year
Annual Operating Hours	5913	5345	3352	h/year
Average Operating COP	3.22	2.88	2.41	[-]
Heat Production Cost	428.29	430.84	440.33	SEK/MWh

The operational envelopes (see Figures 18, 19, and 20) illustrate the dispatch decisions for each configuration based on the hourly production cost. The colour coding indicates whether the heat pump was selected for operation over the biomass boiler. It should be noted that the feasibility shown in these figures is based on variable costs trackable on an hourly resolution, such as electricity spot prices, energy transfer fees, and the price of the alternative (biofuel). Fixed costs and monthly power demand charges are excluded from the hourly dispatch logic, although they are included in the final annual economic outcome (see section 4.5.4). The x-axis in the figures represents the actual temperature lift, in terms of difference between supply and source temperature, as dictated by the specific district heating system and the heat source characteristics. Consequently, the envelopes reflect the heat pump's operational response to the real-world temperature variations encountered during the simulated year.

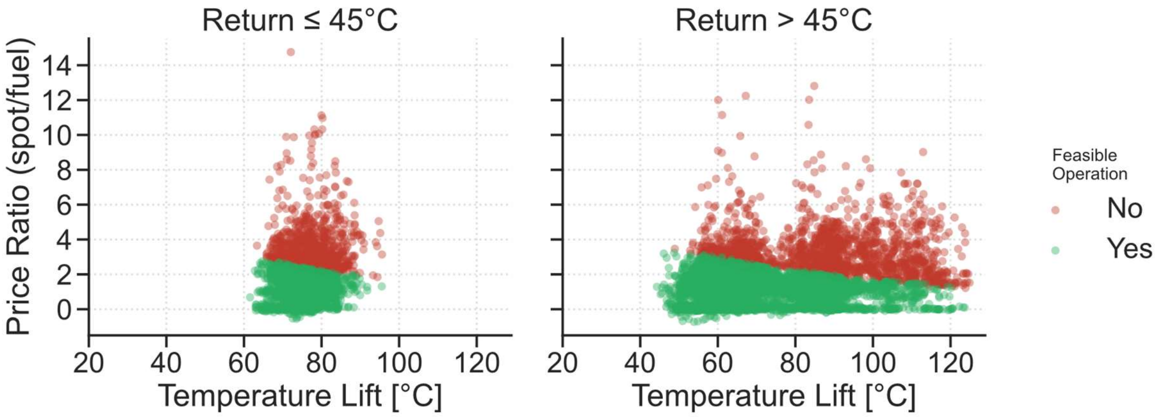

Figure 18: Operational envelope using ammonia as refrigerant.

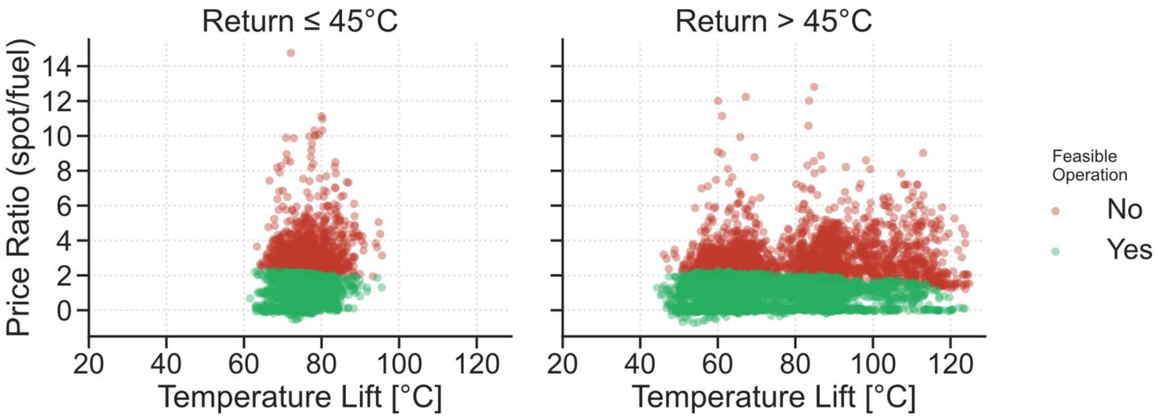

Figure 19: Operational envelope using hydrocarbons as refrigerants.

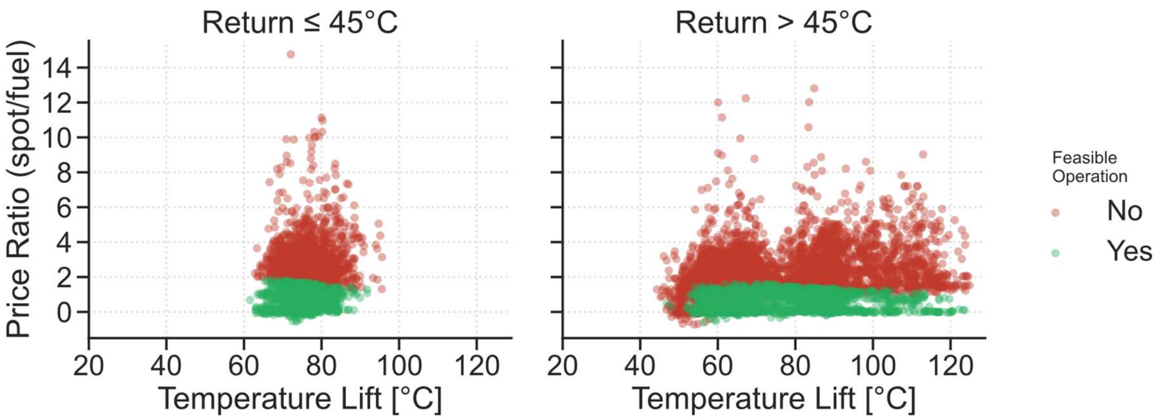

Figure 20: Operational envelope using carbon dioxide as refrigerant.

6.2.2 Electricity Cost Composition

The total expenditure for electricity is primarily driven by variable costs, which constitute the vast majority of the annual budget. As illustrated in Figure 21, fixed costs represent only a small fraction of the total economic burden. The distribution underscores that the operational profitability is heavily dependent on consumption-linked factors rather than static connection fees. A more detailed examination of the variable cost segment, shown in the secondary breakdown in the figure, reveals that electricity tax is the single largest cost driver. The electricity spot price from the day-ahead market follows as the second largest component, being nearly equal in size to the tax. Together, these two elements account for approximately 80% of the total variable expenditure, while the remaining portion consists of energy-based transmission charges and power-related fees. This composition emphasizes that the cumulative impact of taxes and market prices dictates the cost of operation, while the relative impact of grid transmission and power fees remains secondary.

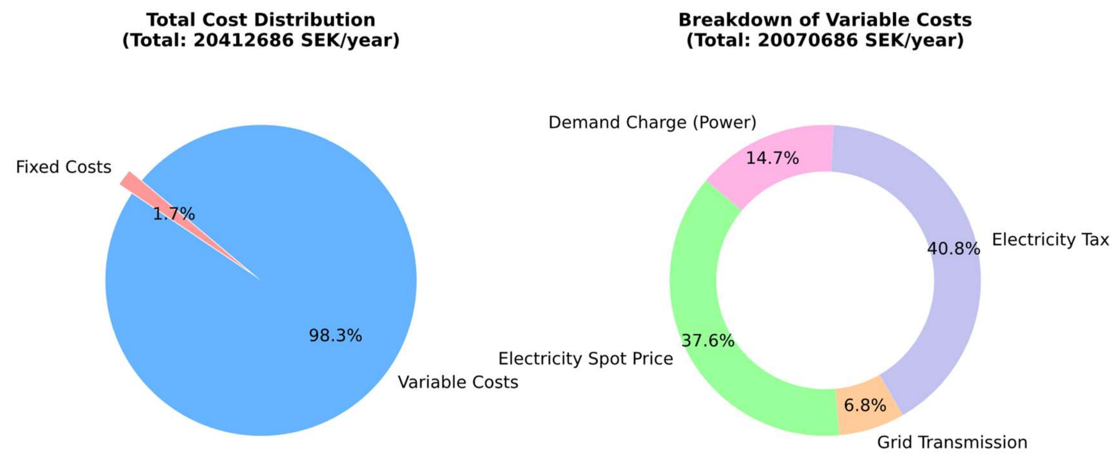

Figure 21: Distribution of total annual electricity costs for the heat pump, using the ammonia cycle.

6.2.3 Investment Potential

Based on the annual net savings and the NPV methodology described in 4.3.5, the justified investment cost for each system has been determined. The results are presented both as a total sum and as a normalized value per kW of installed heating capacity at the predefined design point.

- **Ammonia (R717):** Justified CAPEX of 178.1 MSEK, corresponding to 11,873 SEK/kW.
- **Hydrocarbon Cascade (R600a & R290):** Justified CAPEX of 165.2 MSEK, corresponding to 11,010 SEK/kW.
- **Carbon Dioxide (R744):** Justified CAPEX of 75.0 MSEK, corresponding to 5,000 SEK/kW.

In order to evaluate the numbers derived from the model, a reference point is required. Looking at the material presented in the annex 58 report from the International Energy Agency (IEA), it's stated that high temperature heat pumps have a specific investment cost in the range 200 to 1,500 €/kW related to their maximum supply temperature. The cost range can roughly be translated to 2,200 - 16,500 SEK/kW, using a factor of 11 in currency change. Out of the examples stated in the report, 150 °C in maximum supply temperature is the one most similar to the required maximum supply temperature in the studied case (see Figure 9). The examples of specific investment cost for high temperature heat pumps derived from IEA are highlighted in Table 7, showing that corresponding investment cost for 150 °C in maximum supply temperature is below the justified CAPEX for all investigated configurations.

Table 7: Specific investment cost for high temperature heat pumps [41].

Max. supply temp. [°C]	Spec. inv. cost [SEK/kW]
150	4,400
170	6,600
250	7,700

6.3 Sensitivity Analysis

To evaluate the robustness of the investment and identify the most influential risk factors, a one-way sensitivity analysis was performed on the ammonia case. The results are summarized in Figure 22, which illustrates how sensitive the justified investments are to changes in:

- **Discount Rate**
- **mFRR Price**
- **Minimum Boiler Capacity**
- **Electricity Spot Price**
- **Biofuel Price**

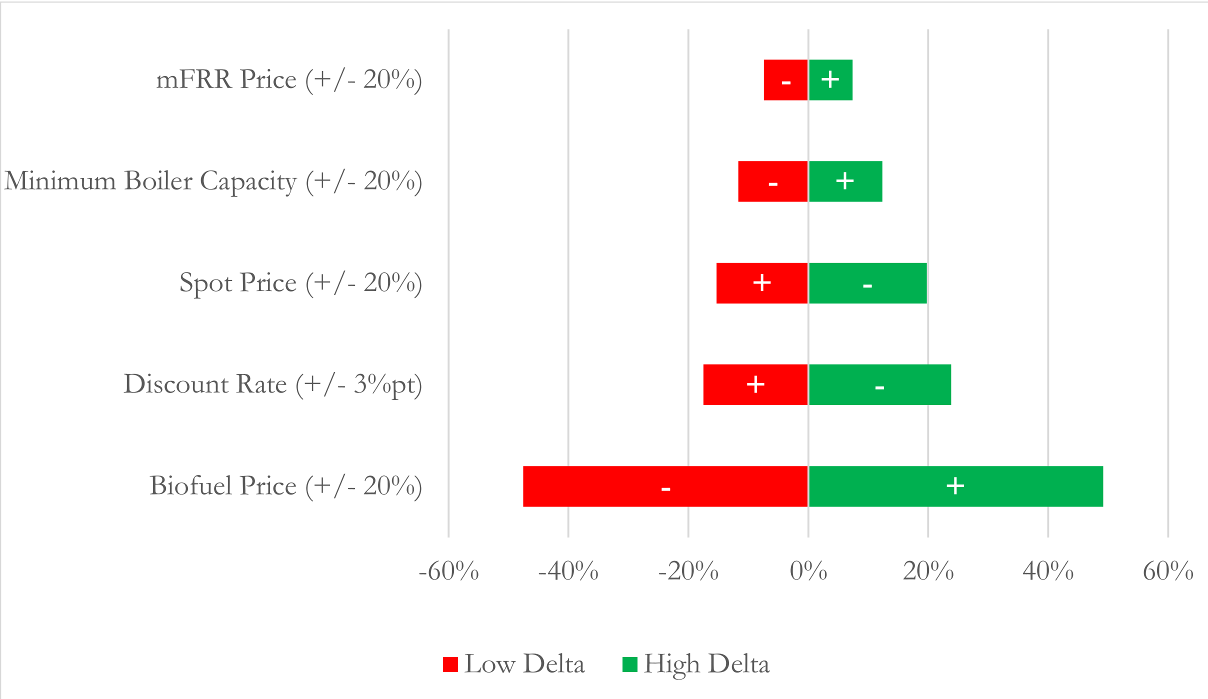

Figure 22: Sensitivity analysis for the ammonia system, with bars representing the change in justified CAPEX relative to the base case (178.1 MSEK).

The sensitivity analysis reveals that the biofuel price is the most influential parameter for the investment potential of the heat pump system. A variation in the cost of displaced fuel results in the widest swing in justified CAPEX. The electricity spot price follows as the second most sensitive factor taking into consideration that the relative change in discount rate is significantly larger compared to the other parameters. While the mFRR revenues and minimum boiler capacity also impact the results, their relative influence is minor in comparison to the price of biofuel.

In addition to these symmetrical parameters, the impact of the district heating return temperature was evaluated through a separate, unidirectional 10 Kelvin reduction. This isolated analysis was conducted exclusively from a network optimization perspective, as assessing an increase in return temperature lacks practical relevance for district heating operators. Lowered return temperature is, on the other hand, advantageous for the heat pump's efficiency. By implementing targeted technical measures such as hydraulic balancing of radiator systems and optimizing substation heat exchangers, the return temperature can be lowered. The results show that the transcritical carbon dioxide cycle is the highly dominant beneficiary of such modification, yielding a substantial increase in justified CAPEX of 117%, driven by an increase in average operating COP by 19.5% (see Table 8). In contrast, the ammonia and cascade configurations exhibit a much lower sensitivity to this variation. The ammonia system shows an increase in justified CAPEX of approximately 12%, while the cascade configuration improves by almost 19%.

Table 8: Economic and technical results with decreased return temperatures.

Metric	Ammonia (R717)	Cascade (R290 & R600a)	Carbon Dioxide (R744)	Unit
Total Net Savings (change)	19.21 (+11.94%)	18.90 (+18.79%)	15.68 (+116.87%)	MSEK/year
Annual Operating Hours (change)	6420 (+8.57%)	5905 (+10.48%)	5158 (+53.88%)	h/year
Average Operating COP (change)	3.43 (+6.12%)	3.09 (+7.29%)	2.88 (+19.50%)	[-]
Justified CAPEX (change)	199.35 (11.93%)	196.14 (+18.73%)	162.79 (+117.05%)	MSEK

7 Discussion

In this section, the most important findings from the results are synthesized and discussed.

7.1 Thermodynamic Analysis

The results presented in Section 6.1 highlight two distinct technical pathways for achieving high performance in large-scale heat pump applications: the two-stage ammonia cycle and the two-stage hydrocarbon-based cascade cycle. The overall robustness of the ammonia system across the investigated scenarios is fundamentally linked to the refrigerant's favourable thermophysical properties, which enable a high thermal capacity while maintaining a low required mass flow rate. From a thermodynamic perspective, this high volumetric capacity minimizes the required mass flow rate, thereby keeping the specific compressor work relatively low and resulting in consistently high performance across the operational regimes. However, the comparative analysis reveals that the technical viability of the hydrocarbon cascade configuration becomes increasingly prominent as the network's temperature lift widens. By splitting a large temperature lift into two separate sub-cycles, the cascade architecture effectively caps the pressure ratios encountered by each individual compressor stage. This directly mitigates the severe volumetric and isentropic efficiency penalties that thermodynamically limit single-stage systems or two-stage systems operating under large temperature lifts. Consequently, the cascade system undergoes a clear thermodynamic optimization at higher temperature lifts, where the reduced pressure ratios allow its cycle efficiency to closely approach the performance of the ammonia system.

Conversely, the analysis underscores the structural vulnerability of the transcritical carbon dioxide system within high-temperature district heating regimes. Unlike ammonia or the hydrocarbon refrigerants, which reject heat through condensation, the carbon dioxide cycle operates above its critical point, rejecting heat progressively via a gas-cooling process. This behaviour shifts the system's efficiency from being primarily source-dependent to heavily return-temperature dependent. When network return temperatures are low, the supercritical fluid can be sufficiently cooled, allowing the transcritical cycle to capture large amounts of low-temperature ambient heat and match the performance of the other cycles at elevated source temperatures. However, as the network return temperature escalates, the gas-cooling process faces a severe thermal bottleneck. The inability to adequately cool the fluid prior to expansion results in an excessively high vapour fraction entering the evaporator, reducing the refrigeration effect and leaving the carbon dioxide system thermodynamically constrained within existing high-temperature networks. The conducted analysis of lowered return temperature showed that while lower temperature offers incremental gains for every configuration by providing more favourable heat rejection conditions, it serves as a critical enabler specifically for the financial viability of the transcritical system.

7.2 Economic Reality

The calculation of the justified CAPEX serves as a critical break-even indicator, defining the upper limit for the investment's financial viability based on the annual operational savings. According to the results in Section 6.2, both the ammonia two-stage system and the hydrocarbon cascade system demonstrate high investment ceilings, with the ammonia system reaching a justified CAPEX of approximately 178 MSEK, compared to 165 MSEK for the hydrocarbon cascade system. Those ceilings are a direct result of the relatively high efficiency achieved by these two-stage configurations. For the ammonia system, the significant economic buffer is necessary to offset the substantial costs associated with its practical implementation. Due to its toxicity and flammability, integrating ammonia into a district heating facility requires stringent safety measures, such as high-capacity ventilation and advanced gas detection, often necessitating a separate building to comply with established directives.

In contrast, the hydrocarbon cascade system offers a different economic profile. While it also utilizes a two-stage approach to reach high temperatures, the use of hydrocarbons which are flammable but non-toxic could potentially streamline the permitting and construction process, especially in urban environments. The fact that the cascade system achieves a justified CAPEX close to the best is a major finding; it shows that the technical complexity of using two different refrigerants could be economically justified by the performance. Consequently, the analysis suggests that the choice between these two leading configurations is not primarily driven by economic potential, as both provide a substantial financial buffer. Instead, the decision should be based on site-specific factors such as local safety requirements, space availability, and the specific risk-management strategies of the utility provider.

7.3 Market Integration

The comprehensive evaluation of the justified CAPEX reveals that the technical efficiency of both the ammonia and the hydrocarbon cascade systems translate directly into robust economic resilience. By establishing maximum investment ceilings in the range 165-178 MSEK, both configurations provide a substantial financial safety margin. This margin is essential for absorbing the high installation and specialized infrastructure costs such as safety systems for toxic or flammable refrigerants associated with large-scale heat pump projects. However, as the sensitivity analysis indicates, the overarching economic viability of all investigated configurations remains inextricably tied to the prevailing price of biofuels. Since the heat pump functions as a partial replacement for an existing biomass-fired boiler, any significant decrease in biofuel price reduces the avoided cost of heat production, thereby challenging the strategic investment case.

Another highly significant finding is the profound impact of the frequency regulation market. The generation of additional annual revenue, totalling approximately 4.8 MSEK for the ammonia system and 5.5 MSEK for the cascade system, acts as an economic lever. This finding carries deep strategic implications: future district heating operators should no longer view large-scale heat pumps solely as static thermal generators. Instead, these assets must be recognized as highly flexible electrical loads capable of providing essential grid stabilization services. It is precisely this dual-revenue stream, combining cost-effective heat production with lucrative grid-balancing services, that renders the investment financially attractive in price-volatile regions such as SE4.

7.4 Uncertainties

A key technical simplification in the simulation model is the assumption of unconstrained capacity regulation for the heat pump compressor. In the model, the compressor frequency is allowed to vary continuously to perfectly match the load or optimize operation against electricity prices. In practical applications, this is limited by the compressor's minimum turn-down ratio and potential stepwise control logic. Consequently, the operational flexibility observed in the results should be viewed as an upper theoretical limit, as real-world mechanical constraints might slightly reduce the ability to follow rapid price fluctuations. Furthermore, the technical requirements for participation in the mFRR market introduce specific challenges depending on the hardware used. Different compressor technologies possess varying capabilities to meet the strict activation time requirements of the balancing markets. This is particularly relevant for ammonia-based systems, which typically employ screw compressors. Due to their mechanical inertia and the complexities of oil management during rapid speed changes, screw compressors operate at the limit of the response times required for mFRR. Therefore, the projected revenues from balancing markets for the ammonia alternative should be interpreted with caution, as additional technical buffers or bidding constraints may be necessary in practice.

Another critical factor is the interplay between the heat pump and the existing biomass boiler. The study assumes a specific minimum load for the biomass boiler, which dictates the available room for the heat pump. Although this parameter was included in the sensitivity analysis, it remains a significant source of uncertainty. A boiler with different flexibility would directly curtail the heat pump's annual full-load hours, as well as the operating expenditure of the alternative (using boiler solely). Thereby impacting the overall net present value of the investment.

8 Conclusion

This thesis has evaluated the technical and economic feasibility of integrating a 15 MW heat pump using natural refrigerants into a district heating network. The following conclusions are drawn based on the results of the modelling and the research questions posed:

In response to the first research question, ammonia remains a highly efficient and robust refrigerant across all investigated temperature conditions, consistently maintaining a high COP. However, the hydrocarbon cascade system demonstrates a more variable performance profile. While it tends to underperform at the extremities of the source temperature range, it achieves an efficiency close to or even equal to ammonia at intermediate temperatures. In contrast, carbon dioxide is the least suitable configuration in these high-temperature scenarios due to its inherent sensitivity to return temperatures. Regarding the second research question, the justified capital expenditure varies between roughly 5,000 and 12,000 in terms of SEK per installed kW at the design point. This threshold is most significantly influenced by the price of biofuels, as this determines the value of the heat being replaced, followed by electricity price volatility and auxiliary revenues from balancing markets.

Finally, in response to the third research question, the study concludes that specific and quantifiable price parity thresholds exist where the production cost of heat for the heat pump aligns exactly with that for biomass combustion. As visualized through the parity analysis in section 6.2.1, these points of economic equilibrium are inextricably linked to the system's COP. Consequently, systems characterized by higher thermodynamic efficiency can tolerate higher electricity-to-fuel price ratios before operation becomes uneconomical. The data in the figures of section 6.2.1 reveals a distinct linear relationship between the maximum acceptable price ratio and the required temperature lift of the system. Specifically, the interface between the profitable operational zones and the uneconomical zones forms a straight line that slopes downward as the temperature lift increases. This indicates that as the gap between the heat source and the delivery temperature widens, the maximum tolerable price ratio decreases proportionally.

In practical terms, for a high-efficiency refrigerant like ammonia, the system can tolerate a price ratio of approximately 2 to 3, meaning electricity spot price can be over two times as much as the biofuel while remaining competitive. However, as the temperature lift increases or as one shifts toward less efficient configurations, this threshold drops toward a ratio of two or lower, significantly narrowing the window for profitable operation. The strategic integration into the mFRR market further bolsters this position by effectively offsetting electricity costs, thereby shifting the parity line and ensuring that large-scale natural refrigerant heat pumps can be a robust, resilient, and viable cornerstone for future electrified district heating in Sweden.

8.1 Future Work

Firstly, while this study utilized a simulation model assuming unconstrained capacity regulation, future research should incorporate dynamic modelling with compressor constraints. Integrating specific performance maps for screw compressors and centrifugal compressors would allow for a more precise evaluation of their ability to meet the sub-minute response times required by the different frequency regulation markets. Such a study could also investigate the role of thermal energy storage in buffering the mechanical limitations of the heat pump during rapid frequency activations.

Secondly, the experimental validation of the hydrocarbon cascade system is a vital next step. While the theoretical results are promising, empirical data on the internal heat exchanger efficiency and oil management in a two-stage hydrocarbon cycle would provide higher certainty regarding its COP. Furthermore, a life-cycle climate performance analysis comparing ammonia with the cascade system would be valuable to quantify the environmental trade-offs between those refrigerants, including potential leakages and energy-intensive component manufacturing.

Lastly, the impact of evolving district heating network characteristics deserves further attention. As networks transition toward the so-called 4th generation district heating with lower supply and return temperatures, the performance gap between carbon dioxide and other natural refrigerants will close. Future studies could model the long-term economic viability of heat pumps in a scenario where return temperatures are actively minimized, potentially altering the strategic recommendation for refrigerant selection.

References

[1] L. Loiacono, L. Rizzo, och C. Stagnaro, ”Impact of bidding zone re-configurations on electricity prices: Evidence from Sweden”, *Energy Economics*, vol. 141, s. 108106, jan. 2025, doi: 10.1016/j.eneco.2024.108106.

[2] M. Moretto och M. G. Pollitt, ”How many zones should an electricity market have? A cross-country perspective on bidding zone design”, *Energy Policy*, vol. 210, s. 115030, mar. 2026, doi: 10.1016/j.enpol.2025.115030.

[3] P. Holmberg och T. P. Tangerås, ”Den svenska elmarknaden─idag och i framtiden”.

[4] G. Klæboe, J. Braathen, A. L. Eriksrud, och S.-E. Fleten, ”Day-ahead market bidding taking the balancing power market into account”, *TOP*, vol. 30, nr 3, s. 683–703, okt. 2022, doi: 10.1007/s11750-022-00645-1.

[5] D. P. Macedo, A. C. Marques, och O. Damette, ”The Merit-Order Effect on the Swedish bidding zone with the highest electricity flow in the Elspot market”, *Energy Economics*, vol. 102, s. 105465, okt. 2021, doi: 10.1016/j.eneco.2021.105465.

[6] ENTSO-e, ”Historical Spot Prices SE1-SE4”. Åtkomstdatum: 13 mars 2026. [Excel]. Tillgänglig vid: https://transparency.entsoe.eu/

[7] J. Jaraitė, A. Kažukauskas, R. Brännlund, C. Kiran, och B. Kriström, ”Intermittency and Pricing Flexibility in Electricity Markets”.

[8] K. Tselika, M. Tselika, och E. Demetriades, ”Quantifying the short-term asymmetric effects of renewable energy on the electricity merit-order curve”, *Energy Economics*, vol. 132, s. 107471, apr. 2024, doi: 10.1016/j.eneco.2024.107471.

[9] S. Zalzar, E. Bompard, A. Purvins, och M. Masera, ”The impacts of an integrated European adjustment market for electricity under high share of renewables”, *Energy Policy*, vol. 136, s. 111055, jan. 2020, doi: 10.1016/j.enpol.2019.111055.

[10] C. Lyu, H. X. Do, R. Nepal, och T. Jamasb, ”Volatility spillovers and carbon price in the Nordic wholesale electricity markets”, *Energy Economics*, vol. 134, s. 107559, juni 2024, doi: 10.1016/j.eneco.2024.107559.

[11] A. Schischke och A. Rathgeber, ”The Impact of Renewables on Spillover Effects in Electricity Markets”, 2025, *SSRN*. doi: 10.2139/ssrn.5144470.

[12] S. Dong, H. Li, F. Wallin, A. Avelin, Q. Zhang, och Z. Yu, ”Volatility of electricity price in Denmark and Sweden”, *Energy Procedia*, vol. 158, s. 4331–4337, feb. 2019, doi: 10.1016/j.egypro.2019.01.788.

[13] X. Malcher och M. Gonzalez-Salazar, ”Strategies for decarbonizing European district heating: Evaluation of their effectiveness in Sweden, France, Germany, and Poland”, *Energy*, vol. 306, s. 132457, okt. 2024, doi: 10.1016/j.energy.2024.132457.

[14] M. Schreiber, M. E. Wainstein, P. Hochloff, och R. Dargaville, ”Flexible electricity tariffs: Power and energy price signals designed for a smarter grid”, *Energy*, vol. 93, s. 2568–2581, dec. 2015, doi: 10.1016/j.energy.2015.10.067.

[15] Vattenfall Eldistribution AB, ”Effekttariffer 2025”. 01 januari 2025. Åtkomstdatum: 16 april 2025. [Online]. Tillgänglig vid: https://www.vattenfalleldistribution.se/globalassets/2.-foretag/abonnemang-och-avgifter/avtal-och-elnatsavgift/prislista-effekttariffer-2025-01-foretag.pdf

[16] Inge Lundqvist, ”A brief description of how Sweden's electricity grid is balanced.” 14 november 2022.

[17] Bo Diczfalusy, ”Ancillary services in the electricity market – Today and in the future”. Energiforsk.

[18] J. E. Feghali *m.fl.*, ”Electrical Grid Flexibility via Heat Pump and Thermal Storage Control”, *IFAC-PapersOnLine*, vol. 55, nr 11, s. 84–89, 2022, doi: 10.1016/j.ifacol.2022.08.053.

[19] Markus Lindahl, ”Flexibility by implementation of heat pumps in thermal networks -Swedish participation in the IEA HPT annex”. Swedish Energy Agency, Boras, 16 augusti 2024.

[20] F. Alsouda, N. S. Bennett, S. C. Saha, F. Salehi, och M. S. Islam, ”Vapor Compression Cycle: A State-of-the-Art Review on Cycle Improvements, Water and Other Natural Refrigerants”, *Clean Technol.*, vol. 5, nr 2, s. 584–608, maj 2023, doi: 10.3390/cleantechnol5020030.

[21] B. Li och A. G. Alleyne, ”A dynamic model of a vapor compression cycle with shut-down and start-up operations”, *International Journal of Refrigeration*, vol. 33, nr 3, s. 538–552, maj 2010, doi: 10.1016/j.ijrefrig.2009.09.011.

[22] N. Li, J. Hou, M. Zeng, T. Ma, P. S. Varbanov, och Q. Wang, ”Dynamic modelling of vapour compression cycles based on an all-mode switchable moving boundary model”, *Applied Thermal Engineering*, vol. 279, s. 127639, nov. 2025, doi: 10.1016/j.applthermaleng.2025.127639.

[23] P. A. Domanski, J. Steven Brown, J. Heo, J. Wojtusiak, och M. O. McLinden, ”A thermodynamic analysis of refrigerants: Performance limits of the vapor compression cycle”, *International Journal of Refrigeration*, vol. 38, s. 71–79, feb. 2014, doi: 10.1016/j.ijrefrig.2013.09.036.
[24] R. M. Singh, A. K. Sani, och T. Amis, ”An overview of ground-source heat pump technology”, i *Managing Global Warming*, Elsevier, 2019, s. 455–485. doi: 10.1016/B978-0-12-814104-5.00015-6.
[25] C. Park, H. Lee, Y. Hwang, och R. Radermacher, ”Recent advances in vapor compression cycle technologies”, *International Journal of Refrigeration*, vol. 60, s. 118–134, dec. 2015, doi: 10.1016/j.ijrefrig.2015.08.005.
[26] Q. D. Yu, ”Theory of energy level and its application in water-loop heat pump system”, *Applied Thermal Engineering*, vol. 119, s. 269–274, juni 2017, doi: 10.1016/j.applthermaleng.2017.03.068.
[27] S. Zhang *m.fl.*, ”The impact of refrigerant leakage on the dynamic operating performance of R600a refrigerator systems”, *Applied Thermal Engineering*, vol. 257, s. 124228, dec. 2024, doi: 10.1016/j.applthermaleng.2024.124228.
[28] I. Boukholda, N. Ben Ezzine, och A. Bellagi, ”Experimental investigation and simulation of commercial absorption chiller using natural refrigerant R717 and powered by Fresnel solar collector”, *International Journal of Thermofluids*, vol. 27, s. 101213, maj 2025, doi: 10.1016/j.ijft.2025.101213.
[29] S. Soni, P. Mishra, G. Maheshwari, och D. S.Verma, ”Comparative energy analysis of R1234yf, R1234ze, R717 and R600a in Vapour Compression Refrigeration system as replacement of R134a”, *Materials Today: Proceedings*, vol. 56, s. 1600–1603, 2022, doi: 10.1016/j.matpr.2022.03.206.
[30] Y. Siva Kumar Reddy, A. M. Guruchethan, S. Kumar Kochunni, S. Singh, M. P. Maiya, och A. Hafner, ”R744 heat pump driven liquid desiccant air conditioning system for hot and humid climates”, *Thermal Science and Engineering Progress*, vol. 56, s. 103079, dec. 2024, doi: 10.1016/j.tsep.2024.103079.
[31] A. Sengupta, P. Gullo, V. Khorshidi, och M. S. Dasgupta, ”Energy and economic comparison of various waste heat-driven cycles for integration with a transcritical R744 supermarket refrigeration system”, *Applied Thermal Engineering*, vol. 288, s. 129555, mar. 2026, doi: 10.1016/j.applthermaleng.2025.129555.
[32] S. Kim, D. Lee, Y. Lee, S. Kwon, och Y. Kim, ”Operating characteristics and design optimization of a heat pump clothes dryer using R290 as an alternative refrigerant to R134a”, *Applied Thermal Engineering*, vol. 279, s. 127609, nov. 2025, doi: 10.1016/j.applthermaleng.2025.127609.
[33] K. Li *m.fl.*, ”Performance study of automotive heat pump system with different refrigerants and leakage combustion characteristics of R290”, *International Journal of Refrigeration*, vol. 180, s. 65–78, dec. 2025, doi: 10.1016/j.ijrefrig.2025.08.019.
[34] A. A. Bani Issa, C. Liang, E. A. Groll, och D. Ziviani, ”Residential heat pump and air conditioning systems with propane (R290) refrigerant: Technology review and future perspectives”, *Applied Thermal Engineering*, vol. 266, s. 125560, maj 2025, doi: 10.1016/j.applthermaleng.2025.125560.
[35] R. Hasan och J. H. Jeong, ”Effects of air impurities on the condensation behavior and thermophysical properties of isobutane (R600a) under typical refrigerator operating conditions”, *International Journal of Refrigeration*, vol. 181, s. 429–448, jan. 2026, doi: 10.1016/j.ijrefrig.2025.11.014.
[36] X. Wang, S. Hu, R. Sun, H. Tian, G. Shu, och Z. Yang, ”Opposite effects of R1234yf on the flammability limits of R600a refrigerant: Experimental and kinetic insight”, *International Journal of Refrigeration*, vol. 183, s. 402–418, mar. 2026, doi: 10.1016/j.ijrefrig.2025.12.018.
[37] H. Averfalk, P. Ingvarsson, U. Persson, M. Gong, och S. Werner, ”Large heat pumps in Swedish district heating systems”, *Renewable and Sustainable Energy Reviews*, vol. 79, s. 1275–1284, nov. 2017, doi: 10.1016/j.rser.2017.05.135.
[38] A. David, B. V. Mathiesen, H. Averfalk, S. Werner, och H. Lund, ”Heat Roadmap Europe: Large-Scale Electric Heat Pumps in District Heating Systems”, *Energies*, vol. 10, nr 4, s. 578, apr. 2017, doi: 10.3390/en10040578.
[39] M. A. Sayegh, P. Jadwiszczak, B. P. Axcell, E. Niemierka, K. Bryś, och H. Jouhara, ”Heat pump placement, connection and operational modes in European district heating”, *Energy and Buildings*, vol. 166, s. 122–144, maj 2018, doi: 10.1016/j.enbuild.2018.02.006.
[40] Swedish Energy Agency, ”Bränslepris skogsflis”. 05 december 2025. Åtkomstdatum: 11 februari 2026. [Online]. Tillgänglig vid: https://www.energimyndigheten.se/statistik/officiell-energistatistik/prisutveckling-inom-energiomradet/tradbransle--och-torvpriser/
[41] IEA, ”High-Temperature Heat Pumps”, HPT-AN58-2, 2023.

TRITA – ITM – EX 2026:352
Stockholm, Sverige 2026

www.kth.se